LOCALIZATION ALGORITHMS FOR PASSIVE TARGETS IN RADAR NETWORKS

by

KARTIK TRASI

Presented to the Faculty of the Graduate School of

The University of Texas at Arlington in Partial Fulfillment

of the Requirements

for the Degree of

MASTER OF SCIENCE IN ELECTRICAL ENGINEERING

THE UNIVERSITY OF TEXAS AT ARLINGTON

May 2007

ACKNOWLEDGEMENTS

I would like to acknowledge my grandmother, parents, relatives and friends for their constant support and encouragement, and my supervising professor Dr. S. Tjuatja for his patience and guidance.

December 10, 2006

ABSTRACT

LOCALIZATION ALGORITHMS FOR PASSIVE TARGETS IN RADAR NETWORKS

Publication No. _____

Kartik Trasi, M.S.

The University of Texas at Arlington, 2007

Supervising Professor: Dr. Saibun Tjuatja

Despite the recent advances in location discovery for sensor networks the robustness of the algorithms needs more consideration. In this study, we propose an improved, robust algorithm for passive targets in radar networks. Robust, fault tolerant, localization algorithms are essential for accurate position estimation of targets in wireless sensor networks. The objective of this research is to provide a numerical and experimental validation for localization of a single passive target in an indoor environment.

TABLE OF CONTENTS

LIST OF ILLUSTRATIONS

Figure Page

LIST OF TABLES

Table Page

CHAPTER 1

INTRODUCTION

1.1. Localization in Radar Networks

1.1.1 Overview

The basic purpose of a radar based location sensing is to detect the presence of the object of interest by transmitting an electromagnetic signal and detecting, in the unavoidable system noise. If the backscattered wave is of adequate signal to noise ratio it will provide ranging information of the target under consideration. In most of the developments, the targets are assumed to be point targets. This is not an undue idealization since a target will behave as if the radar cross section is concentrated into a point whenever the target is small in terms of the resolution capability of the waveform. The matched filter or correlation radar is a type of radar in which the receiver is designed for optimum signal detection in Additive White Gaussian Noise. In this kind of receivers, the impulse response of the receiver is the same shape except for a reversal on the time axis. The receiver essentially measures the degree to which the received signal and the transmitted signals are correlated with each other [23].

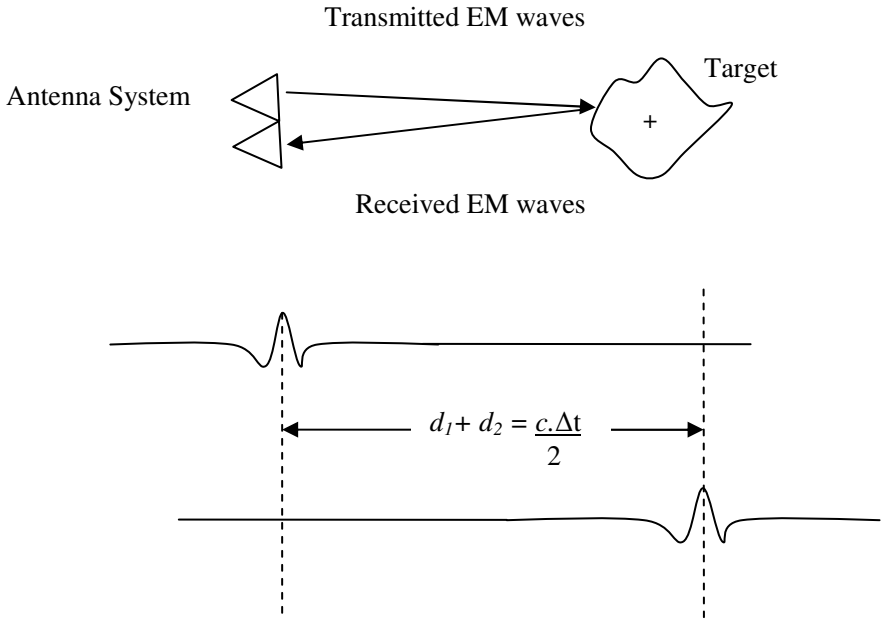

Figure 1.1: Distance Estimation using Time Difference of Arrival

There are various techniques for Passive and non-cooperative Ranging range estimation. Range estimation is basically measurement of distance between two points. Range may be estimated by Radar Signal Strength (RSS) based on the Path loss model.

$$PL(d) = \left[PL_0 + 10\gamma \log_{10} \left(\frac{d}{d_0} \right) \right] + S; \quad d \geq d_0$$

(1.1)

However, RSS is not preferred for the experimental purposes since it is extremely problematic for fine-grained, ad-hoc applications. RSS depends on Path loss characteristics which depends on the environment ($1/r^n$), Shadowing depends on environment, Short-scale fading due to multipaths adds random high frequency component with huge amplitude (30-60dB) [36] especially for indoor environment. The Time Difference of Arrival (TDoA) technique is used for range estimation for the localization experiment.

The range estimates from the different reference sources is routed to a centralized location where a decision is made. A co-operative centralized algorithm reduces excessive computational overhead on the individual nodes. The existing centralized systems for localization attempt to solve the problem of localization using different approaches based on the available hardware, signal propagation models, timing and energy requirements, and the nature of the environment. The accuracy of the localization algorithm is a function of node density, time synchronization of devices and calibration of the system. [1]

The time control subsystem generates synchronization timing signals required throughout the radar system. A modulated signal is generated and sent to the antenna by the modulator or the transmitter block. Switching the antenna between the transmitting and receiving modes is controlled by the duplexer. The duplexer allows one antenna to be used as both transmit and receive. The range in meters is defined as

$$R = \frac{c\Delta t}{2} \qquad (1.2)$$

Where c is the speed of light and factor 0.5 is to account for the two way time delay. In general, a pulsed radar transmits an receives a train of pulses. The Inter Pulse Period (IPP) is T, and the pulse width is τ. The IPP is also known as the Pulse Repetition Interval (PRI).

Range resolution is a metric that describes its ability to detect targets in close proximity to each other as distinct objects. Radar systems are normally designed to operate between a minimum range and maximum range. The distance between R_{max} and R_{min} is divided into M range bins of length ΔR each.

$$M = (R_{\max} - R_{\min}) \Big/ \Delta R \qquad (1.3)$$

$$\Delta R = R2 - R1 = c\frac{(t2 - t1)}{2} = \frac{c}{2B} \qquad (1.4)$$

In the real-world environment, the propagation losses in the severe multi-path causing environment impose challenges on the design of a scalable, easily deployable, and computationally inexpensive and a robust position estimation system. The designed system should ensure the following [8]:

a) The algorithm should be robust enough to tolerate multiple network failures. The failures may be due to malicious nodes in the network or the error may be induced by the environment.

b) The algorithm should be scalable. That means it should be practical easily extensible to a large network.

c) The algorithm should be computationally inexpensive so that the nodes used in the network may have limited capabilities.

d) It should be applicable for practical environments including indoor and outdoor.

The algorithms take different approaches to solve the problem of target position estimation. These algorithms differ in the assumptions and their required of accuracy and computation and processing complexity and the number of nodes available for co-operative location estimation.

1.1.2 Contribution

In this study, we propose an improved, robust algorithm for passive targets in radar networks. The main objective of this work is to improve the localization accuracy of the algorithm based on signal properties in combination with robust graphical techniques. We present a numerical approach and an experimental validation of the modified algorithm.

1.1.3 Related Work

The triangulation algorithm (also known as the minimum mean square error (MMSE) estimation algorithm) has been used widely in wireless sensor networks for co-operative location sensing in the past. It is the basis of position estimation in satellite-based GPS systems. However, MMSE method is sensitive to range estimation errors from individual nodes. Hence, the performance of the algorithm largely depends on the accuracy of the nodes. In a network, nodes may report spurious readings due to noisy data which results in error in the position estimation. Robustness of the algorithm can limit the mean square error of the location estimate to a certain extent. The Iteratively Refined - Minimum Mean Square Estimate (IR-MMSE) method presented by Liu *et al* in [7] to mitigate range estimation errors by eliminating the inconsistent

data. A graphical technique has been called the Hough Transform Inspired algorithm (HTIA) has been formulated for multiple targets in wireless sensor networks by C.Chang *et al* [4],[5]. A Grid Based technique has been studied by Fretzagias *et al* in [8] has been implemented on Mica2 motes [7].

CHAPTER 2

LOCALIZATION

2.1 Algorithms

Based on the requirements, implementation-specific constraints of a sensor network, a basic set of performance metric may be devised. For specific applications, only a subset of the criteria may be relevant [20]:

1. Accuracy: in location sensing accuracy is of maximum primary importance. However, accuracy may be directly associated with the complexity and the convergence time of the algorithm. Hence, an optimum balance between must be established based on the application requirements.

2. Error tolerance: range measurement errors may occur due to the low signal to noise ratio (SNR) of the received signals to perform ranging. Also low sampling rates may induce measurement errors.

3. Convergence time: Applications may need fast convergence times, for example becomes critical if the target is mobile, or the reference nodes themselves are in motion.

2.1.1 Minimum Mean Square Estimate (MMSE)

The basic idea behind MMSE is that if the distance (d) between a node and the target is known, then locus of the target must is on a circle centered at the node and with radius d and the target lies at the point where all the circles intersect. Localization based solely on the Euclidean distance information d from a minimum of $n + 1$ sensors where n is the n-dimension localization.

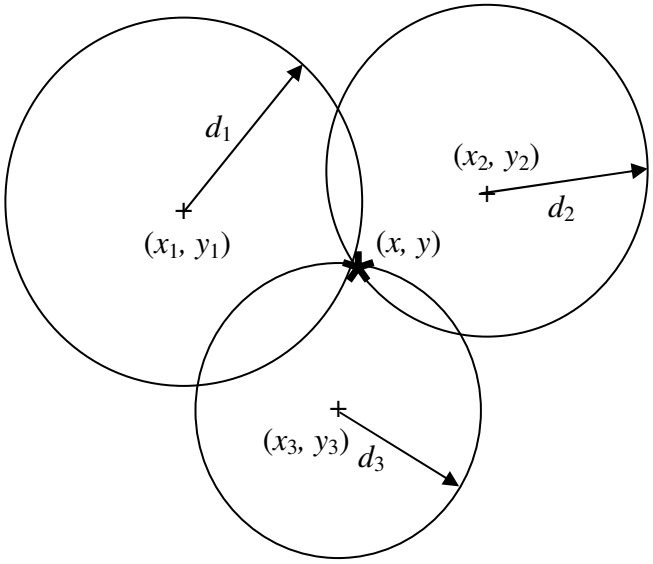

Figure 2.1: Concept of localization using MMSE algorithm

Let (x, y) be the actual position of the target and (x_o, y_o) be the estimated location of the target and (x_i, y_i) for i=1…n are the co-ordinates of the reference nodes. The range estimate is d_i by the n nodes.

$$\begin{bmatrix} (x_1 - x)^2 + (y_1 - y)^2 \\ \vdots \\ (x_n - x)^2 + (y_n - y)^2 \end{bmatrix} = \begin{bmatrix} d_1^2 \\ \vdots \\ d_n^2 \end{bmatrix} \quad (2.1)$$

These nonlinear equations relating the unknown coordinates to the distances and reference point coordinates can be solved in a number of ways. To reach the closed form solution, one can start by subtracting the First line in the above equations from each of the remaining equations. This yields a linear system of n - 1 equations, which can be written as

$$Au = b \quad (2.2)$$

Where,

$$A = \begin{bmatrix} (x_1 - x_2)^2 & (y_1 - y_2)^2 \\ \vdots & \vdots \\ (x_1 - x_n)^2 & (y_1 - y_n)^2 \end{bmatrix} \quad (2.3)$$

$$u = \begin{bmatrix} x \\ y \end{bmatrix} \quad (2.4)$$

$$b = 0.5\begin{bmatrix} d_2^2 - d_1^2 - x_2^2 + x_1^2 - y_2^2 + y_1^2 \\ \vdots \\ d_n^2 - d_1^2 - x_n^2 + x_1^2 - y_n^2 + y_1^2 \end{bmatrix} \quad (2.5)$$

This system of equations is over-determined if n ≥ 4. For the case if there are no ranging errors any four of the n - 1 total equations can be selected and used for the triangulation operation. Again assuming no errors on the range measurements using 4 or n - 1 equations would not yield any additional information. In this case the unknown position can be computed using

$$u = A_4^{-1} b_4 \quad (2.6)$$

Where A_4 and b_4 are any four rows of A and b.

However when range measurements are noisy and $n > 4$ then selecting any 4 equations would not all yield the same solution. In this case the availability of the additional reference points can be used to the advantage [20]. The over-determined system of equations can be solved using a least squares solution. This is a technique borrowed from linear algebra that is often used in applications that consists of over-determined systems with noisy measurements.

$$u = (A^T A)^{-1} A^T b \quad (2.7)$$

The method is called the Least Square solution and the vector $A_p = (A^T A)^{-1} A^T$ is called the pseudo inverse of A such that $u = A_p b$.

Inputs: (x_{si}, y_{si}) - Known Sensor locations ('Anchors'), d_{si} - Range Estimation from Sensor i,Outputs: (x, y)

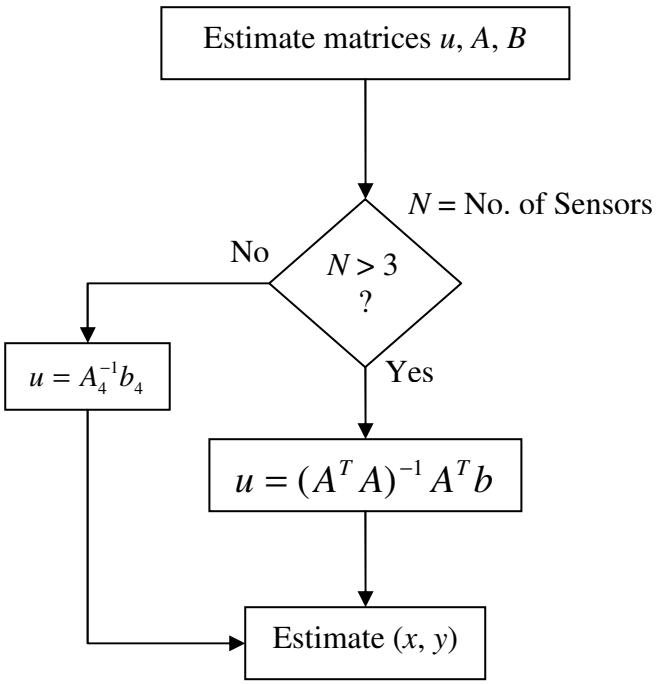

Figure 2.2: MMSE Flow Chart

2.1.2 Iteratively Refined – Minimum Mean Square Estimate (IR - MMSE)

Iteratively Refined – Minimum Mean Square Estimate Algorithm is a refined triangulation features the capability to eliminate inconsistent estimates. Let (x, y) be the actual position of the target and (x_o, y_o) be the estimated location of the target and (x_i, y_i) for i=1…n are the co-ordinates of the reference nodes. The range estimate is d_i by the n nodes.

Given set of location references $\ell = \{(x_1, y_1, d_1), (x_2, y_2, d_2), ...(x_n, y_n, d_n)\}$. The location estimation based on l has a mean square estimation of

$$\zeta^2 = \sum_{i=1}^{m} \left(d_i - \sqrt{(x_o - x_i)^2 + (y_o - y_i)^2} \right) \leq \gamma^2 \qquad (2.8)$$

ζ^2 is a good indicator of inconsistent location references. The threshold γ^2 depends on the measurement error model. [7]

Inputs: (x_{si}, y_{si}) - Known Sensor locations ('Anchors'), d_{si} - Range Estimation from Sensor i, Outputs: (x, y)

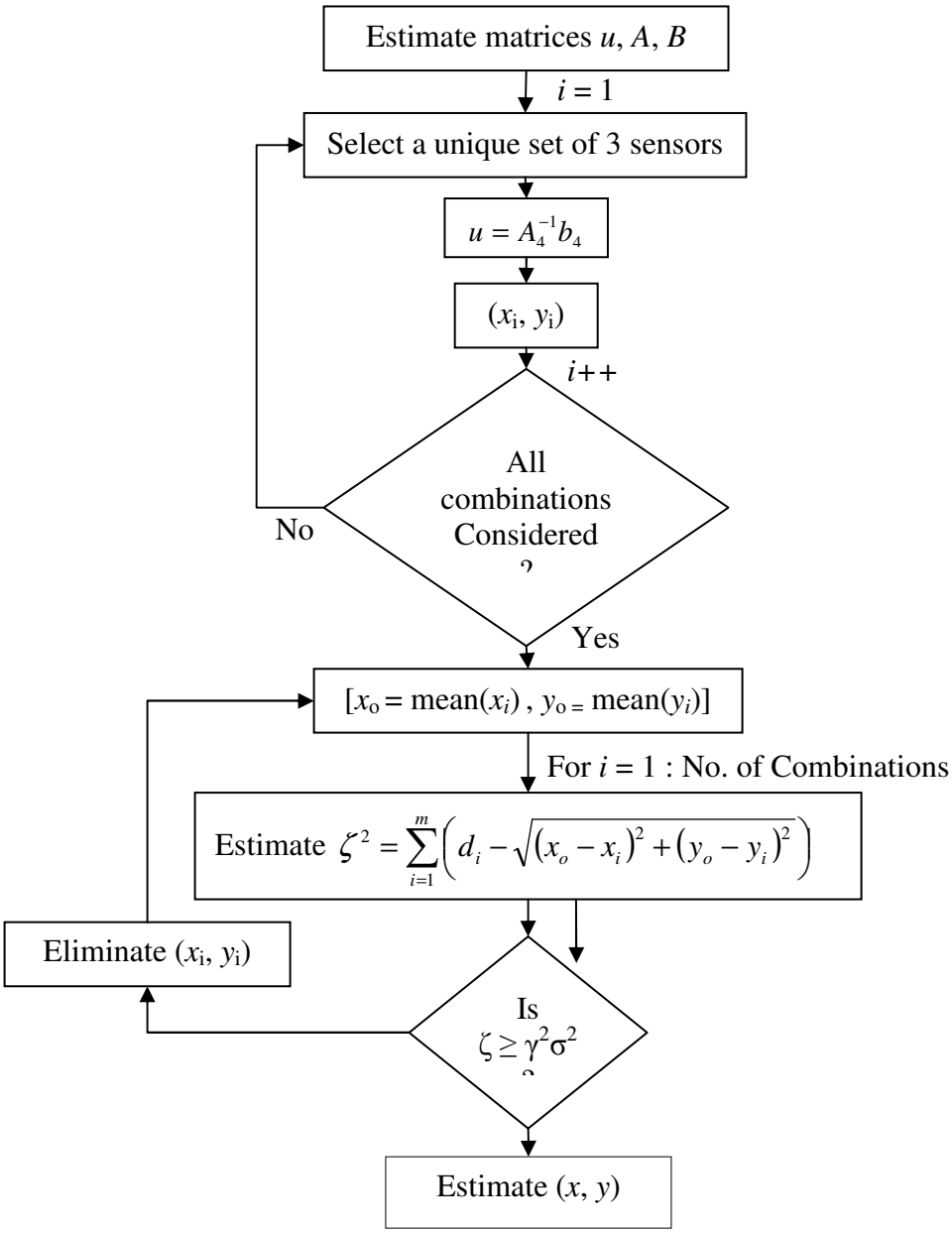

Figure 2.3: IR-MMSE Flow Chart

2.2 Grid Based Algorithms - Graphical Techniques for Localization

2.2.2. Hough Transform Inspired Algorithm [4]

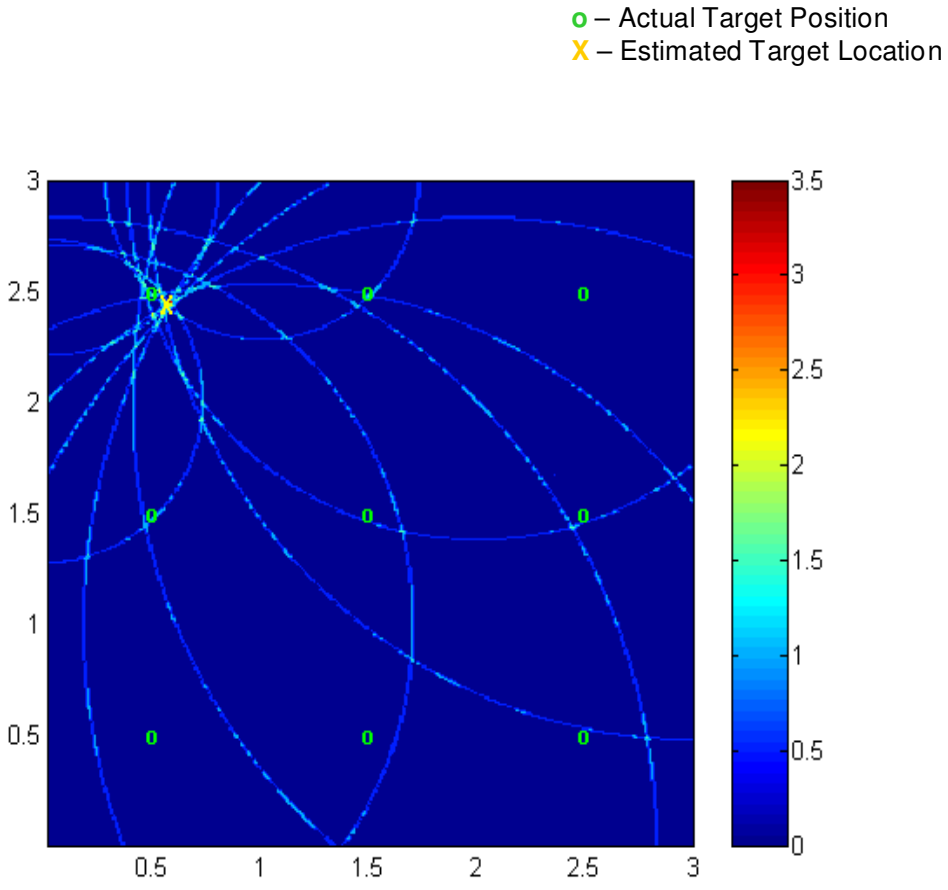

Figure 2.4: Hough Transform inspired Localization Algorithm

2.2.2.1. Survey of Hough Transform and its Applications

The Hough Transform has been developed by Paul Hough in 1962 and patented by IBM. It became in the last decade a standard tool in the field of artificial vision for the detection of straight lines, circles and ellipses. The Hough Transform is predominantly robust to noisy data. It can also be extended to non-linear characteristic relations and made resistant to noise by use of anti-aliasing techniques [30]. Hough Transform has become popular in the recent past for

The Hough transform is a standard method in finding some geometric structures from a noisy image. Given a noisy image as the input from the image space, the Hough transform is trying to find the line structures in the dual space of line equations. Given the multi-path distances, the point on the dual space (2D space) with large likelihood is determined by maximizing the score function.

Cheng *et al* [4] present a localization algorithm inspired by the Hough Transform [14]. The concept behind Hough Transform is to discretize a bounded space and then search for optimal solutions on the grids. We can apply the same basic concept to the localization problem; we can assume the objects are in a bounded 2D space. Further, we can solve the grid for optimal graphical solution based on certain constraints. The algorithm is stated below.

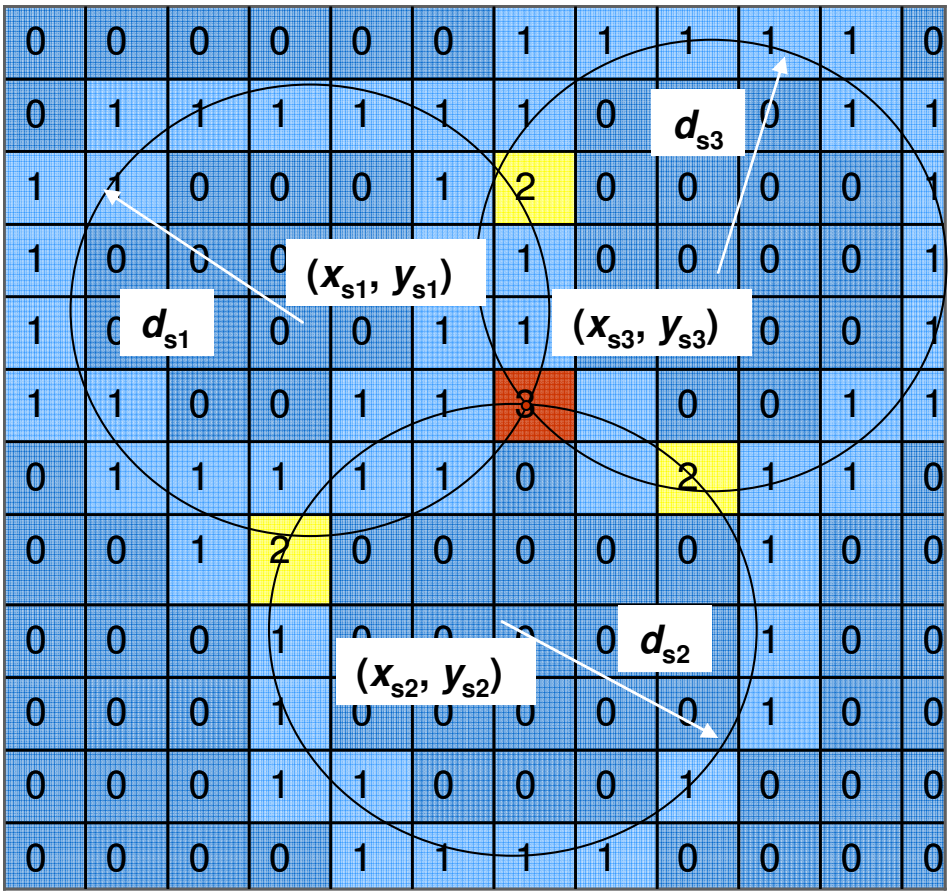

Figure 2.5: Hough Transform Inspired Algorithm

Inputs: (x_{si}, y_{si}) - Known Sensor locations ('Anchors'), d_{si} - Range Estimation from Sensor i; Outputs:(x, y)

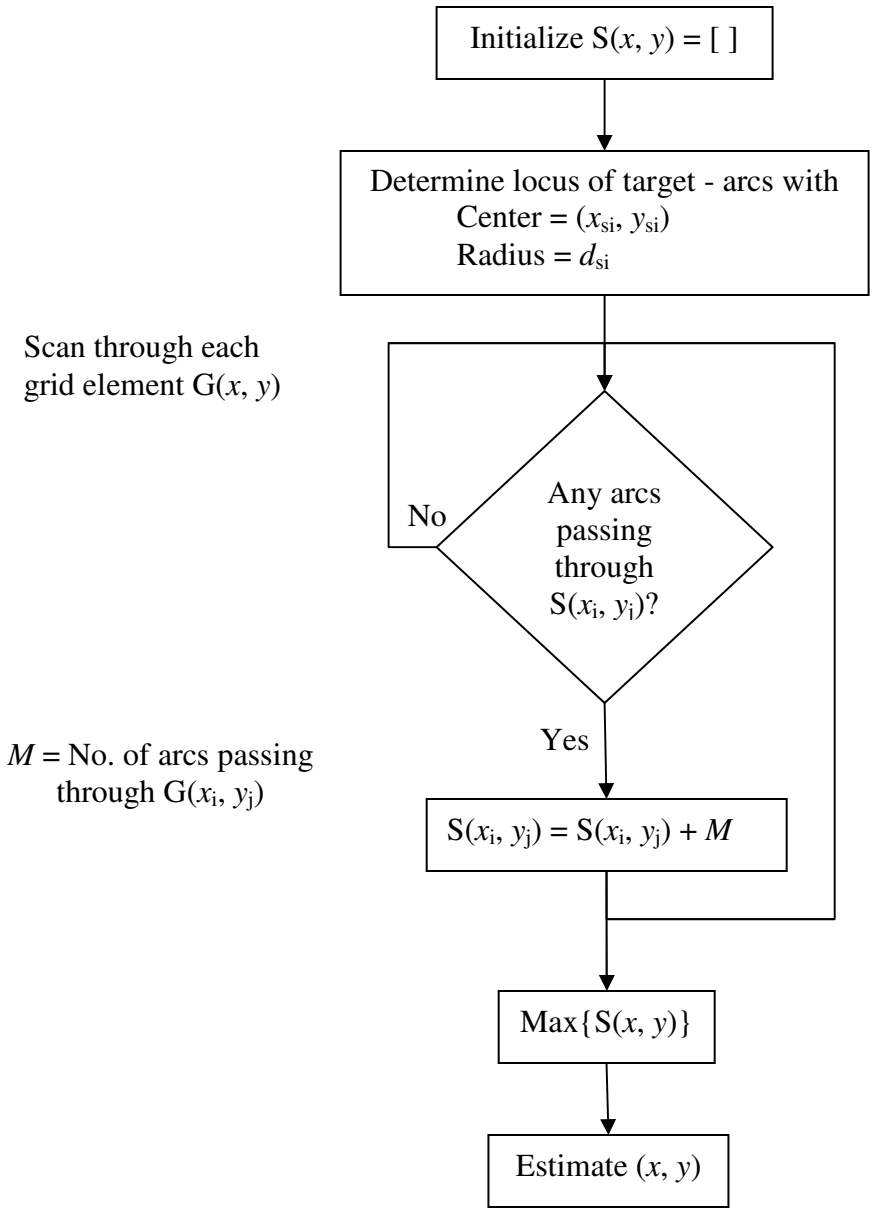

Figure 2.6: Hough Transform Inspired Algorithm Flow Chart

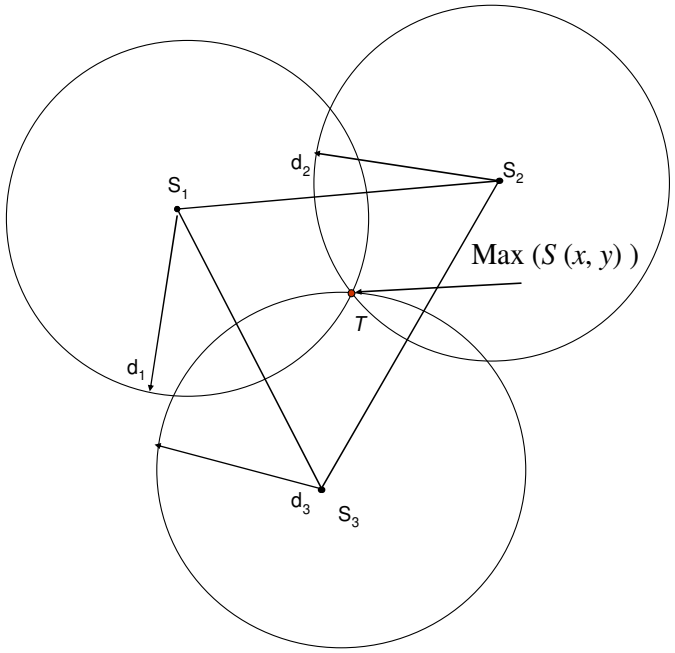

Figure 2.7: Hough Transform Inspired Algorithm for Ideal Range Estimates

The above figure shows sensors with ideal range estimates. The locus of the target is an arc from each of the 'anchor' centers and the range estimates as the corresponding radii. The estimated target location is (labeled 'T' in the diagram) is the grid point which contains all the arc intersections as obtained by maximizing the score function.

2.2.2.2. Limitations of Hough Transform Inspired Algorithm

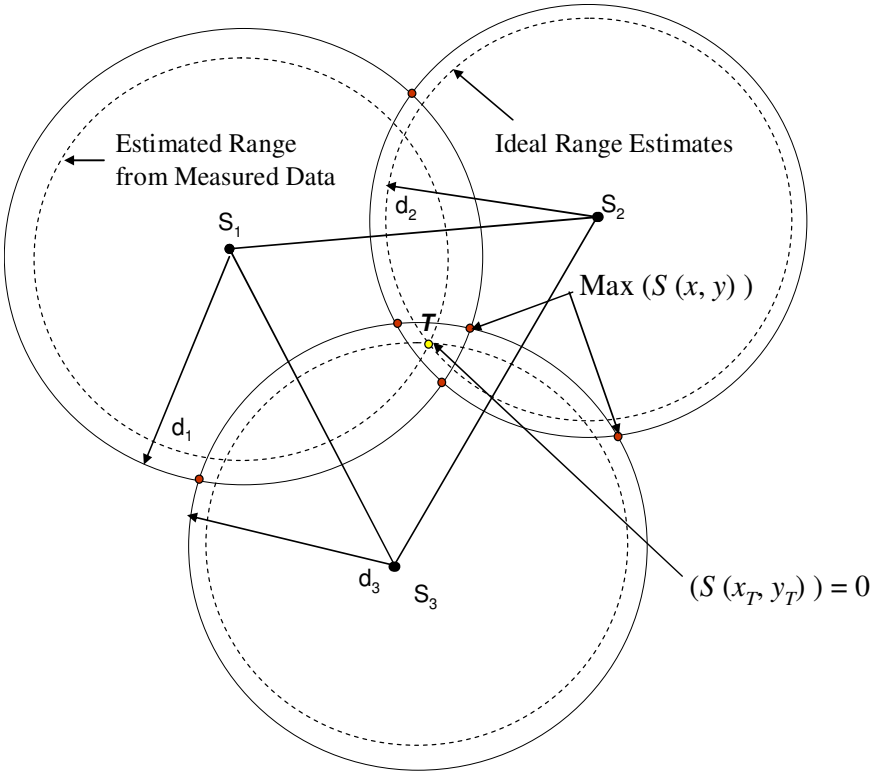

Figure 2.8: Limitations of Hough Transform Inspired Algorithm

The Hough Transform Inspired Algorithm fails for a single target when the Max{S(x, y)}is not unique. In other words, maximum score function occurs at more than one grid point. For comparison purposes, we find the centroid of the grid points at which the Max{S(x, y)} occurs as shown below.

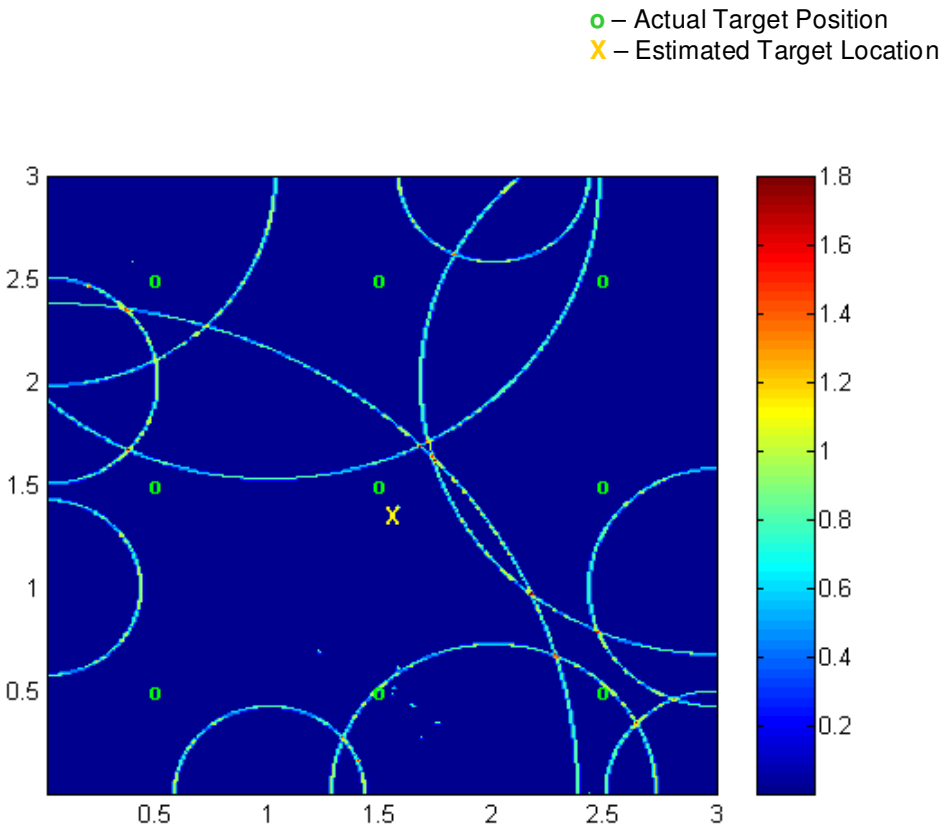

Figure 2.9: Hough Transform Inspired Algorithm for Noisy Range Estimates

2.2.2. “Voting Process” (VP) – Grid Based Location Estimation [8]

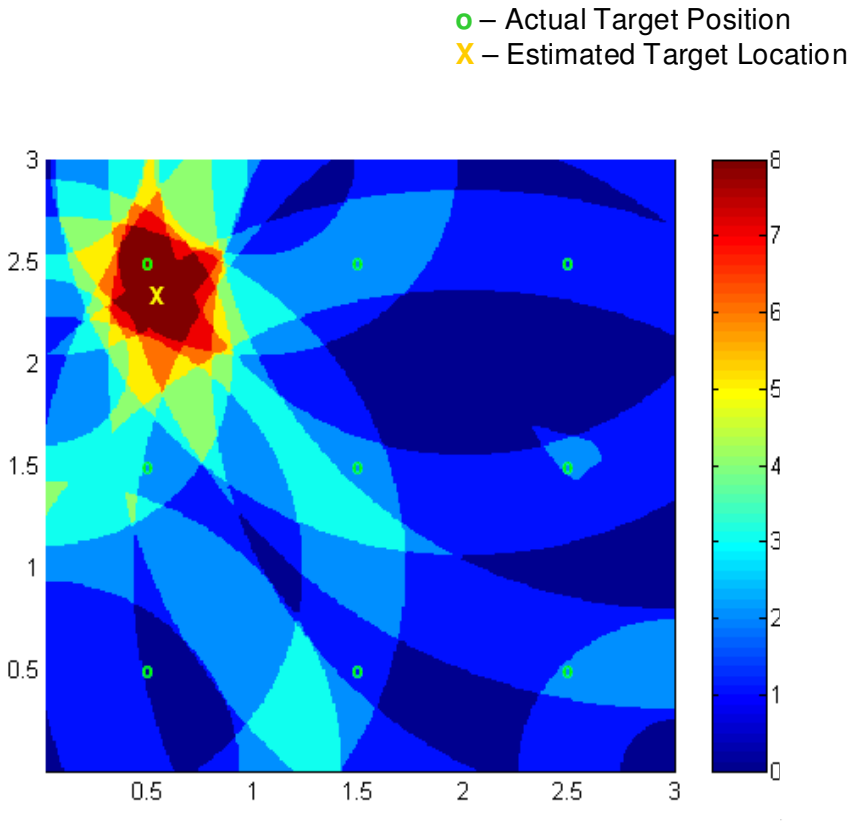

Figure 2.10: “Voting Process” (VP) – Grid Based Location Estimation

Fretzagias et al present a Voting Based algorithm that represent as the grid that the central processing node $s(x, y)$ maintains during a run and the value of the cell (x, y). The value of a cell reflects the likely position of the target.

At each run, each gathers the range information and updates the information at the central node and the central node computes the target location. The algorithm

reduces to the Hough Transform Inspired Algorithm when $d_i^l \approx d_i^u$. The reference nodes reporting large range estimation errors can be eliminated since it does not overlap the Max{S(x,y)} region. In other words, since the candidate ring usually does not overlap the maximum likelihood region the range estimate is ignored.

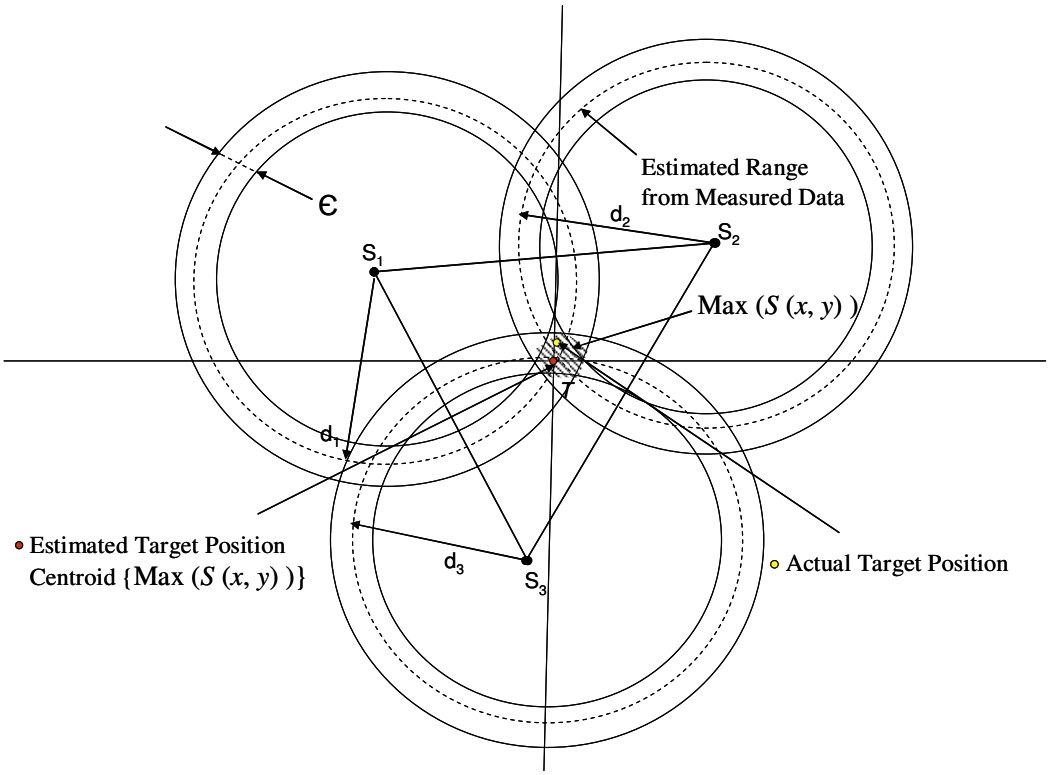

Figure 2.11: Target localization using Voting Process

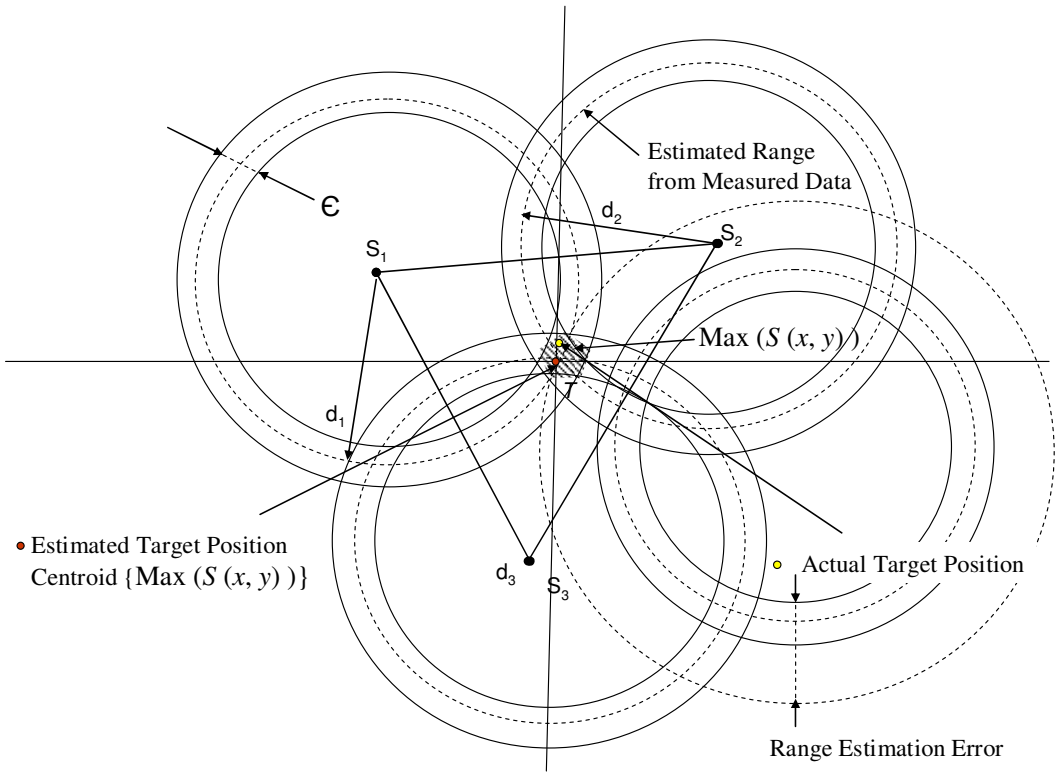

Figure 2.12: Elimination of Range Estimation Errors using Voting Process

Inputs: (x_{si}, y_{si}) - Known Sensor locations ('Anchors'), d_{si} - Range Estimation from Sensor i; Outputs:(x, y)

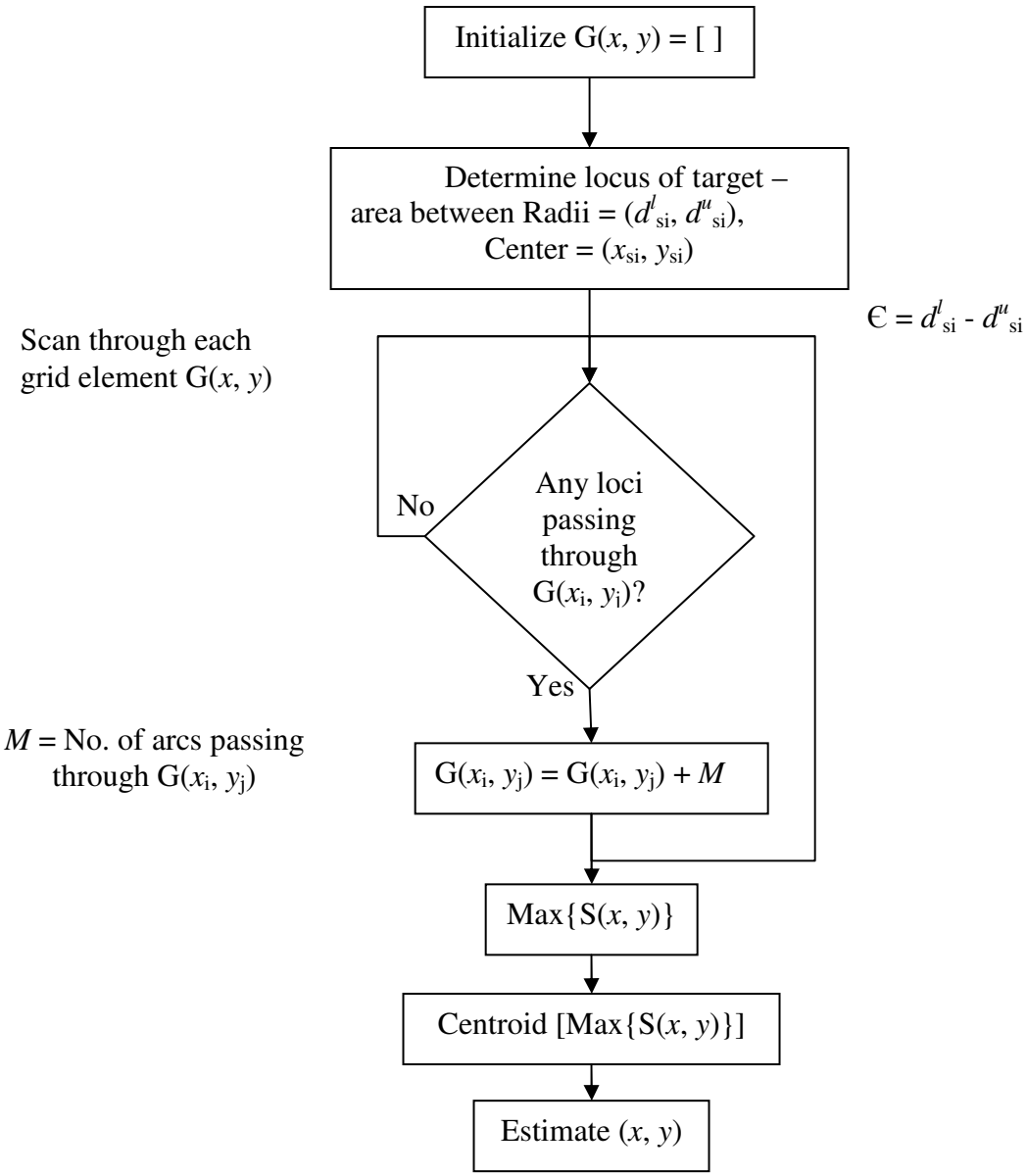

Figure 2.13: Voting Algorithm Flow Chart

2.2.3. Modified - Grid Based Algorithm

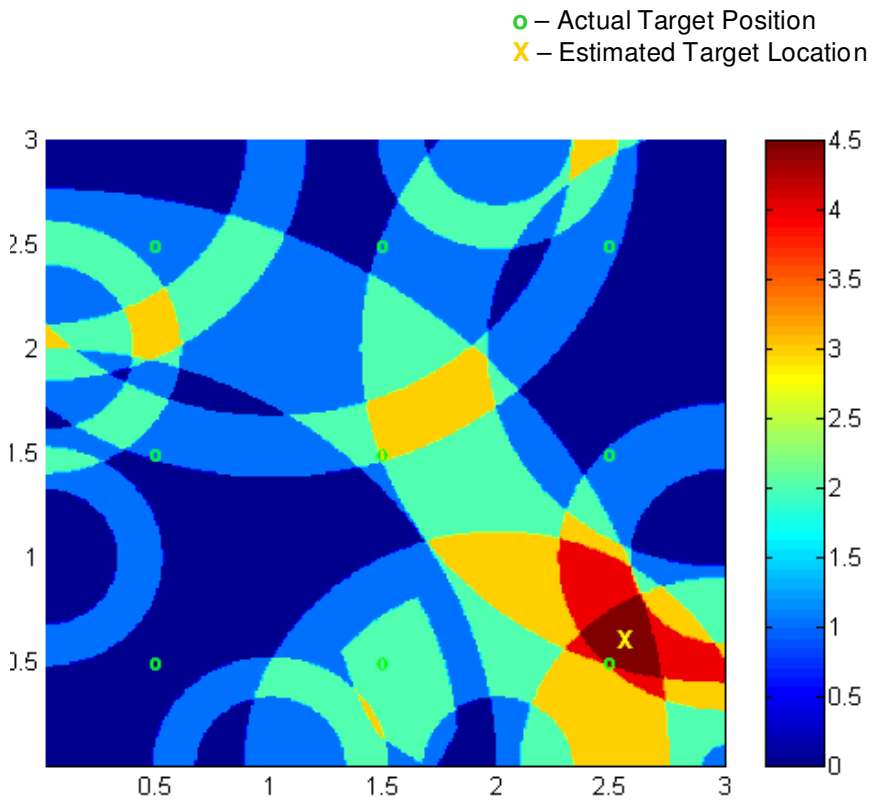

Figure 2.14: Target Localization using Modified - Grid Based Algorithm

The values of the d_i^l and d_i^u may be dynamically calculated using the correlation of the range measurement signal received at each sensor with the reference (training sequence) signal used for measurement calibration. Highly correlated with the training sequence has a greater difference between d_i^l and d_i^u (i.e. large value of ∂ where $\varepsilon = d_i^u - d_i^l$) which implies a thicker candidate ring and signals with lower

correlation will have a smaller value of ε corresponding to a narrower candidate ring. Uncorrelated signals will have $d_i^l = d_i^u$ hence the candidate ring will have zero width and the reference node will be completely eliminated.

Inputs: (x_{si}, y_{si}) - Known Sensor locations ('Anchors'), d_{si} - Range Estimation from Sensor s, Outputs: (x, y)

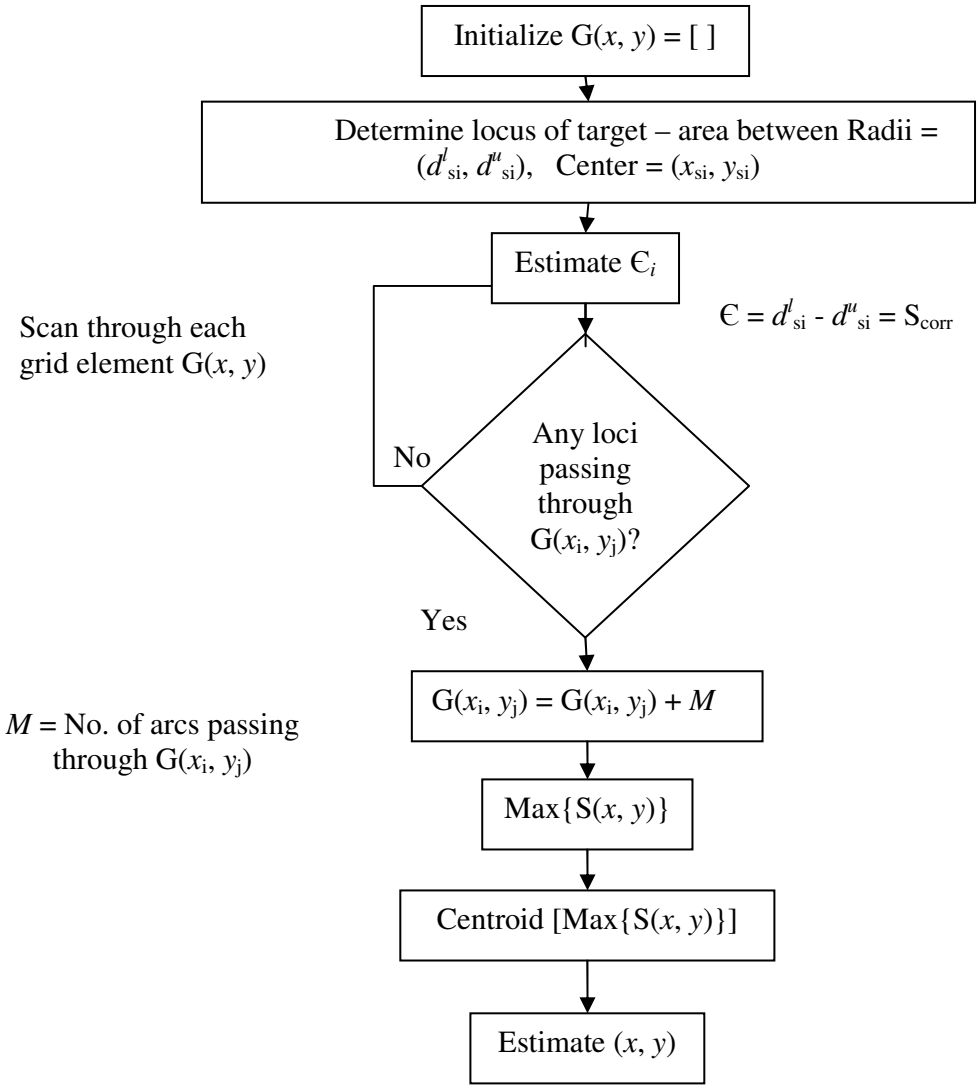

Figure 2.15: MGBA Flow Chart

CHAPTER 3

SIMULATION STUDY

.In our simulation, we generate 12 sensors with known locations known as 'anchors' and 9 target locations as shown in the geometry below as used in the experimental study. The sensors with known positions are known as anchors.

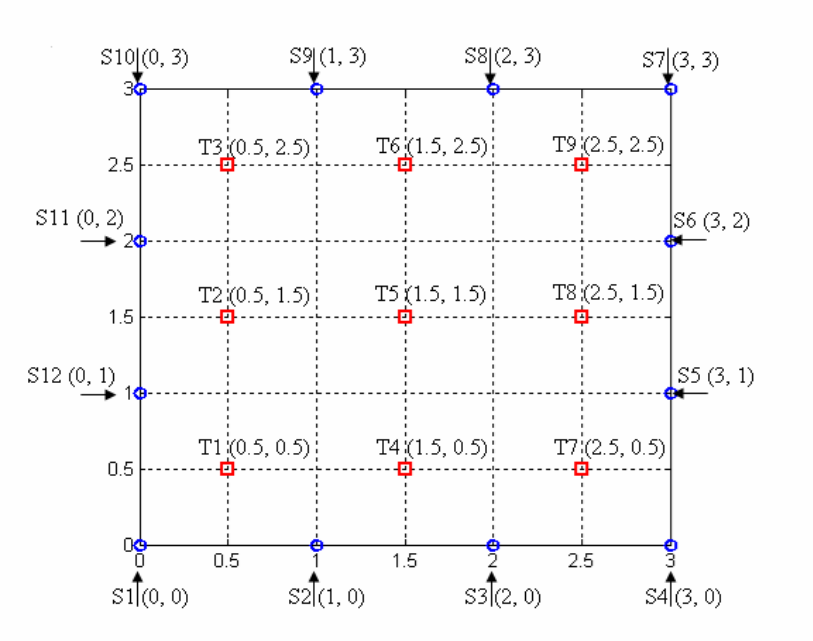

Figure 3.1: Simulation Geometry

The algorithms are evaluated in three different error distributions in range estimations among sensors. The simulation procedure involves estimating the ideal range estimates from each from the sensors to the actual targets. Assuming that these range estimates are corrupted by Gaussian Noise with a mean that is determined by the error distribution and the variation determined by the mean range estimation among the sensors plotted across the x-axis.

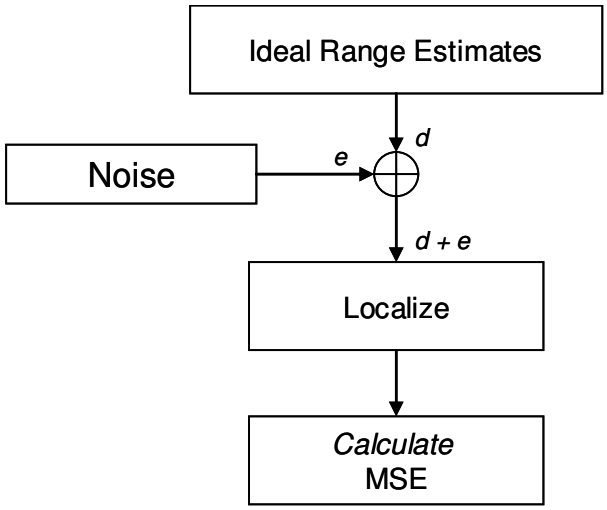

Figure 3.2: Simulation procedure

The simulation study is divided into three scenarios based on the error distribution. The correlation of the signal is used as the reliability parameter for each of the sensors. For the case when the $\mu = 0$, the all sensors are equally set to be reliable. This case is applicable to the high SNR case when the range estimation errors are not a function of distance. The sensors are equally affected by noise. In the second case, mean $\mu = f(d)$, which is when the sensors closer to the target are more reliable. The first

two cases are applicable to omni-directional antennas. In the third case, $\mu = f(d,\theta)$ which implies that the sensors closer to the target and closer to the antenna axis are more reliable. This case is applicable to directional antennas.

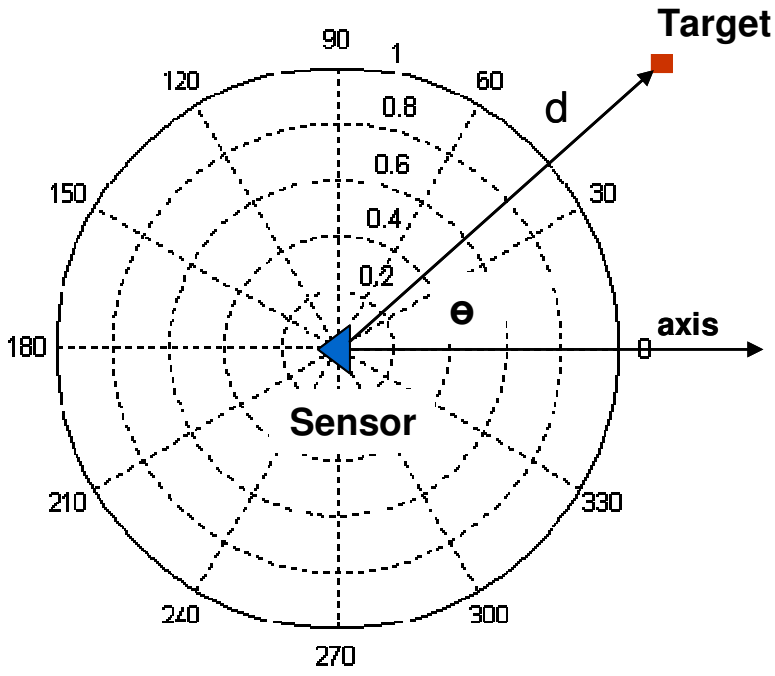

Figure 3.3: Sensor – Target geometry

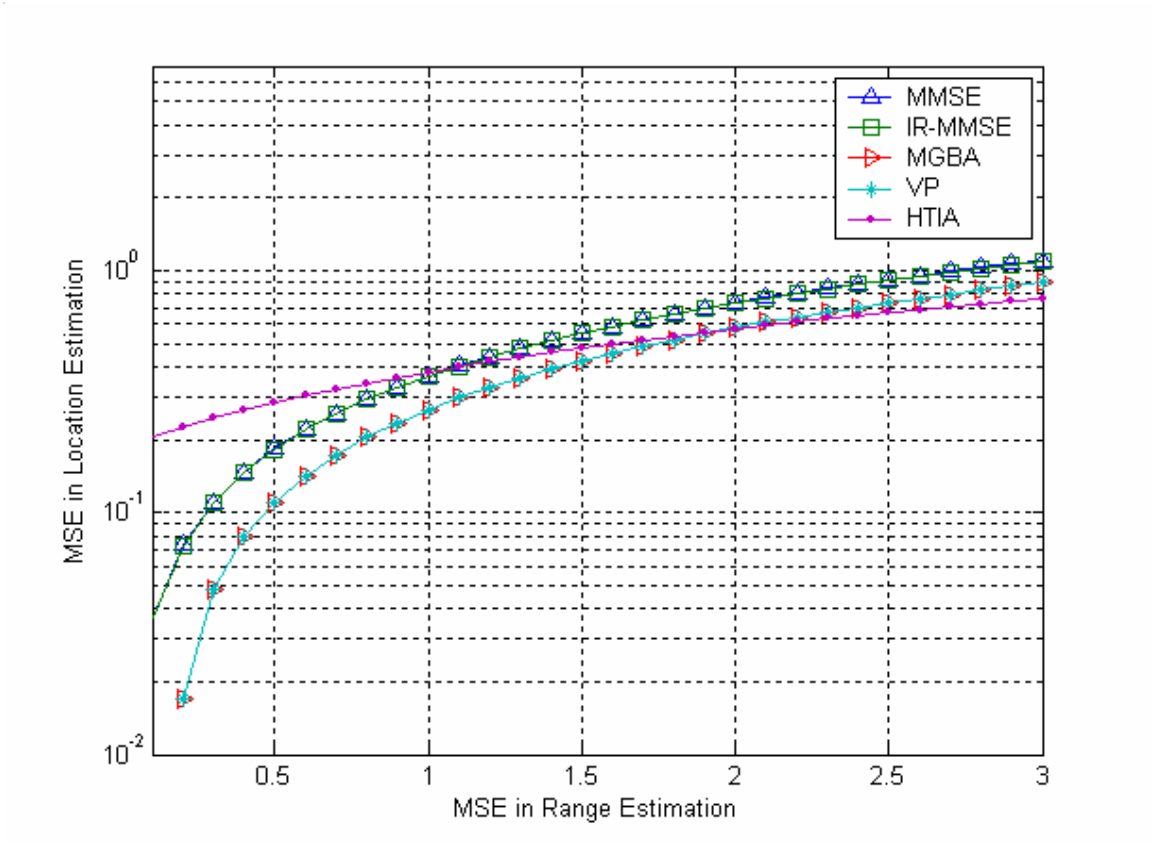

Figure 3.4: MSE in location estimation for Range Estimation Error N (0, σ^2)

This scenario simulates a high SNR case wherein all the sensors are equally affected by noise. The range estimates are equally corrupted by noise ($\mu = 0$). As seen in the above figure, the graphical techniques perform better than the traditional MMSE algorithms.

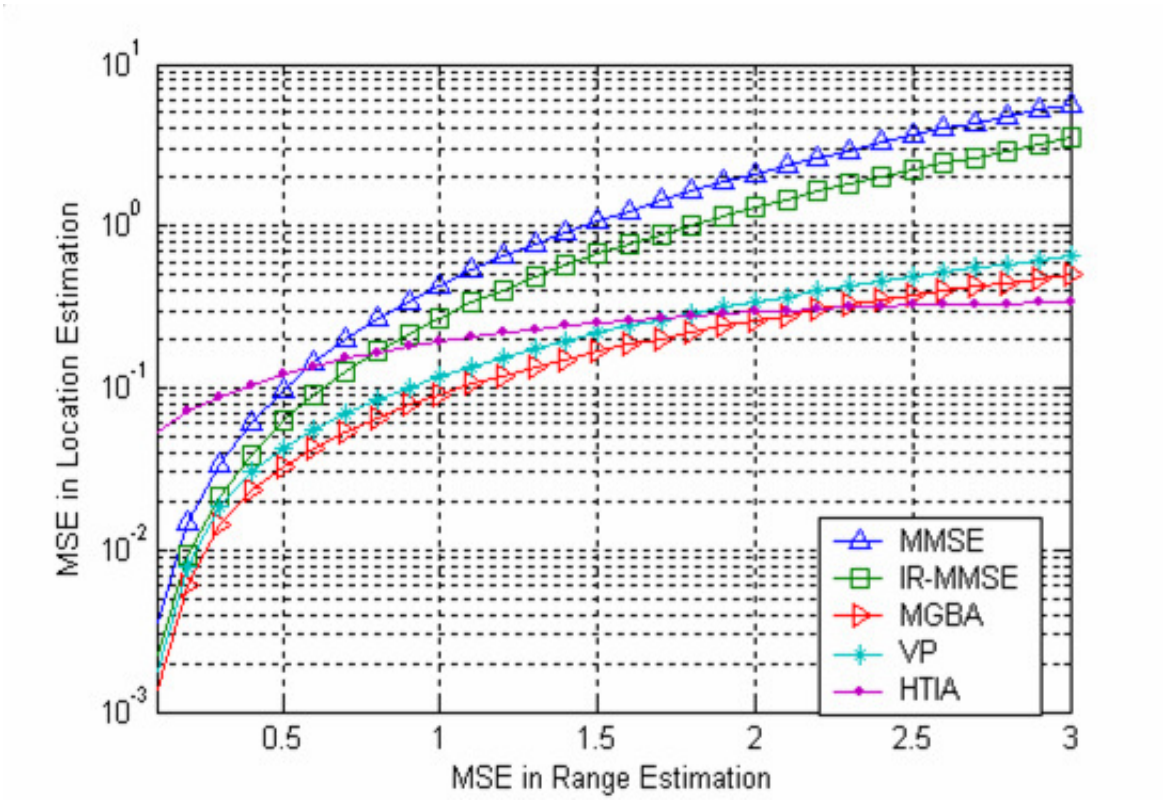

Figure 3.5: MSE in location estimation for Range Estimation Error N (μ, σ^2), μ = f (d)

This scenario simulates a high SNR case wherein all the sensors are not equally affected by noise. The sensors further away from targets have noisier range estimates as compared to the targets closer to the sensors. The sensors closer to the target have a better SNR since the backscatter from the target is larger and the nose floor is the same. The range estimates are equally corrupted by noise ($\mu = f(d)$). As seen in the above figure, the graphical techniques perform with a better accuracy in this case. This can be

explained by the non-uniform error distribution. The non-uniform distribution allows better filtering of consistent data from the spurious ones. The robustness of the graphical techniques is illustrated by improvement at larger mean square range estimation errors. In Case 3, the mean is given as $\mu = f(d, \theta)$ which imples Sensors closer to the target and closer to the antenna axis are more reliable. This case is applicable when the sensors are directional antennas

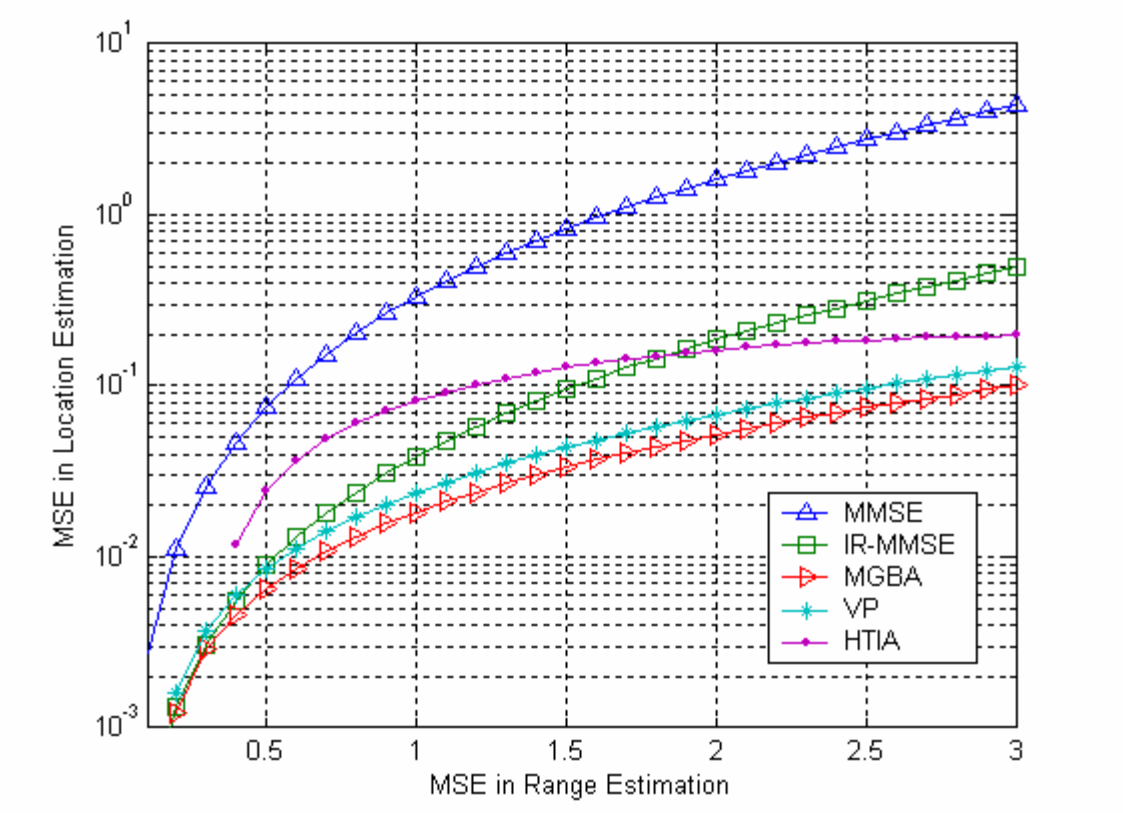

Figure 3.6: MSE in location estimation for Range Estimation Error N (μ, σ2), μ = f (d, ɵ)

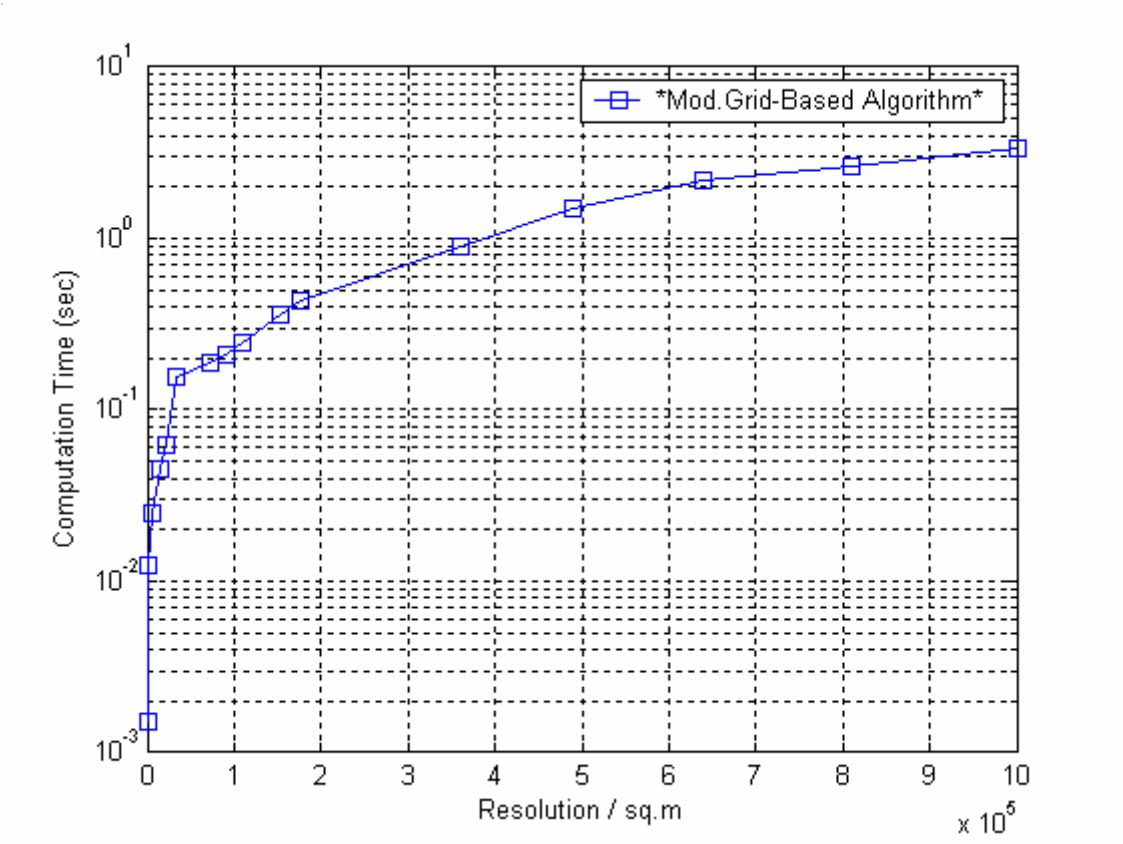

Figure 3.7: Computation Overhead

The graphical techniques have a major limitation of computational and storage overhead. As the resolution of the grid (M x M) increases the complexity and the computational efficiency increases rapidly. The memory size required to store the score function also increases appreciably with the increasing resolution. The accuracy of the algorithm is a function of resolution. However, there has to be a trade-off between the computational efficiency and accuracy.

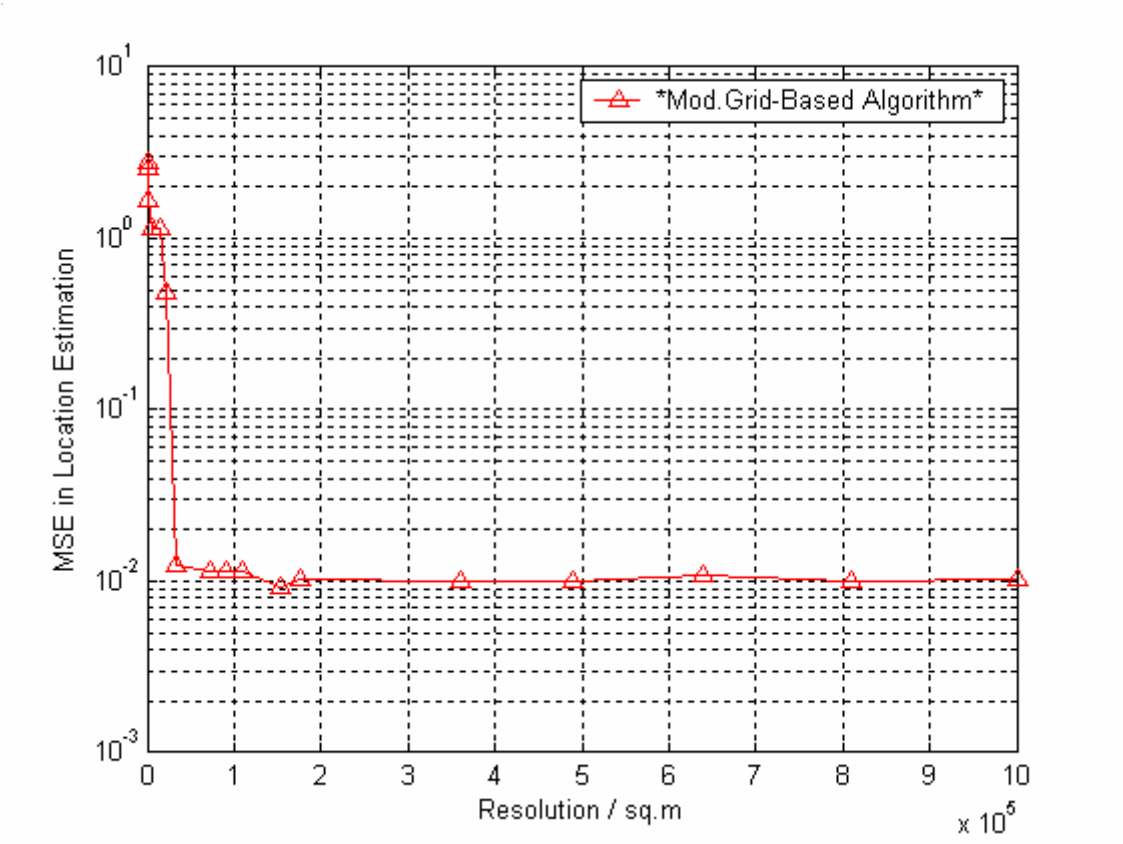

Figure 3.8: Accuracy as a function of Resolution

The above figure illustrates the accuracy with increasing resolution. The larger resolution reduces the quantization error hence improving the overall accuracy of the algorithm. However, this improvement in the accuracy comes with the cost of increased complexity, larger storage requirements and increased computation time.

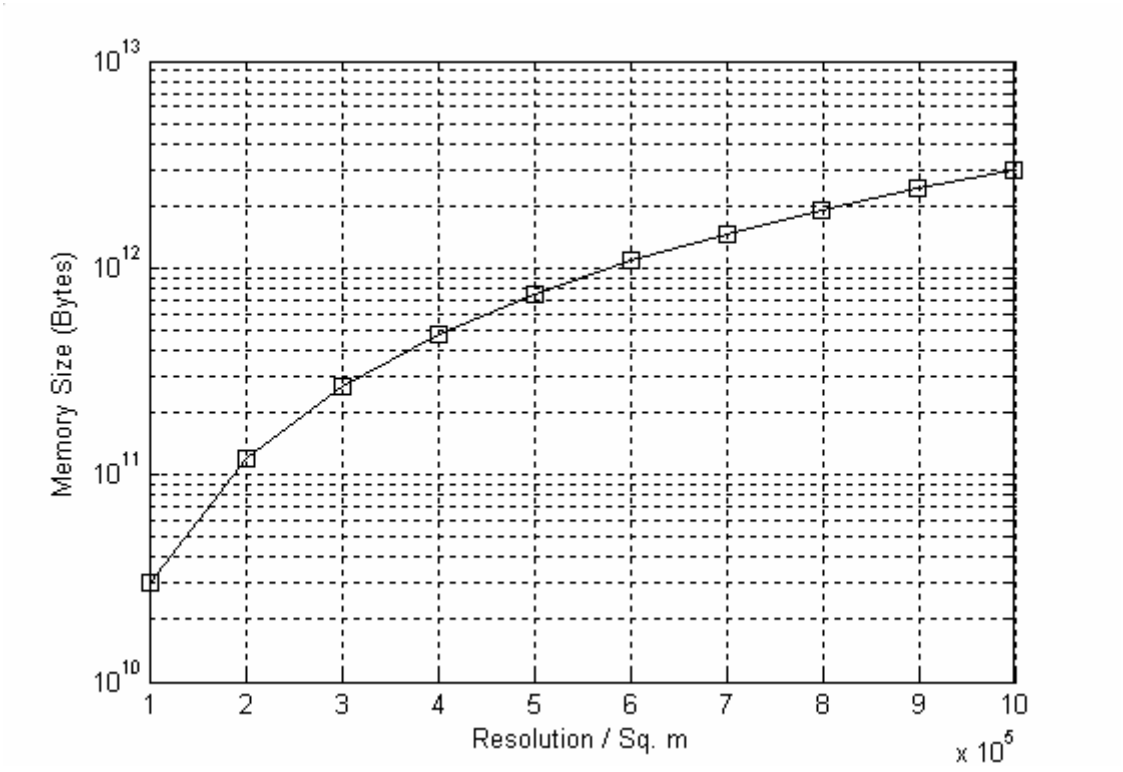

Figure 3.9: Storage Overhead as a function of Resolution

Finding the optimal parameters and estimating the number of iterations is a complex problem. One of the solutions to this optimization problem as mentioned by Chang *et al.*[40] is to use the coarse (low resolution) to fine technique (high resolution) in which the conventional Hough Transform is performed in a low resolution parameter space to obtain a rough detection first, then the accurate detection can be obtained subsequent increase in the resolution. The optimum solution is obtained by estimating a threshold function which decides the optimum threshold between computational efficiency, storage overhead and the accuracy of the algorithm.

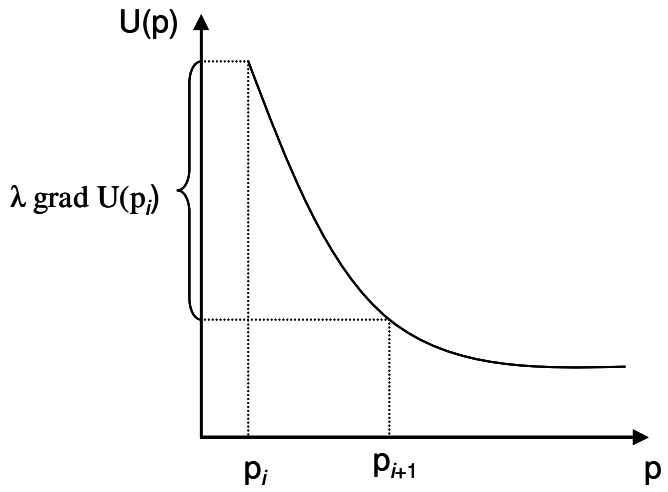

Figure 3.10: Evaluating the optimization function

The accuracy of the final solution depends on many parameters like signal characteristics obtained at the sensors and the range estimation accuracy at the sensor level. A simplified problem statement is to obtain the optimum value of the resolution which provides acceptable accuracy for the application and further increasing the resolution does not affect the accuracy of the algorithm by a significant amount. This change in the accuracy for each increment in the resolution is given by the gradient as mentioned in the flowchart.

Suppose the algorithm can be described by an equation with p parameters as follows:

$$f(a_1, a_2, a_3, \ldots, a_p, x, y) = 0; \qquad (3.1)$$

In the Hough Transform, the parameter space is divided into M x M cells, supposing the same quantum m is used for all the parameter calculations. The voting value $U(a_{1i}, a_{2i}, \ldots, a_{pi})$ at the point p_i is given by

$$\frac{\partial U}{\partial a_1} = 0; \frac{\partial U}{\partial a_2} = 0; \frac{\partial U}{\partial a_3} = 0; \cdots, \frac{\partial U}{\partial a_p} = 0; \qquad (3.2)$$

We can obtain a number of extreme values of U and the corresponding optimal parameters.

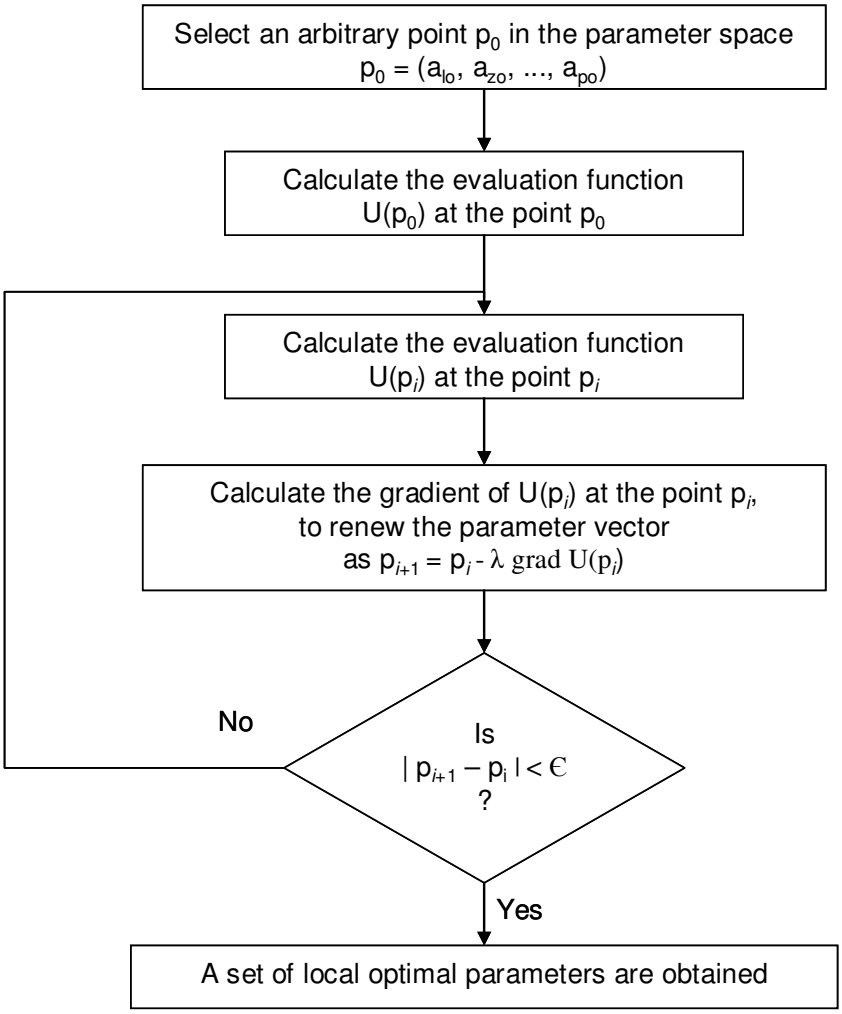

Figure 3.11: Optimization Flowchart

CHAPTER 4

EXPERIMENTAL ANALYSIS

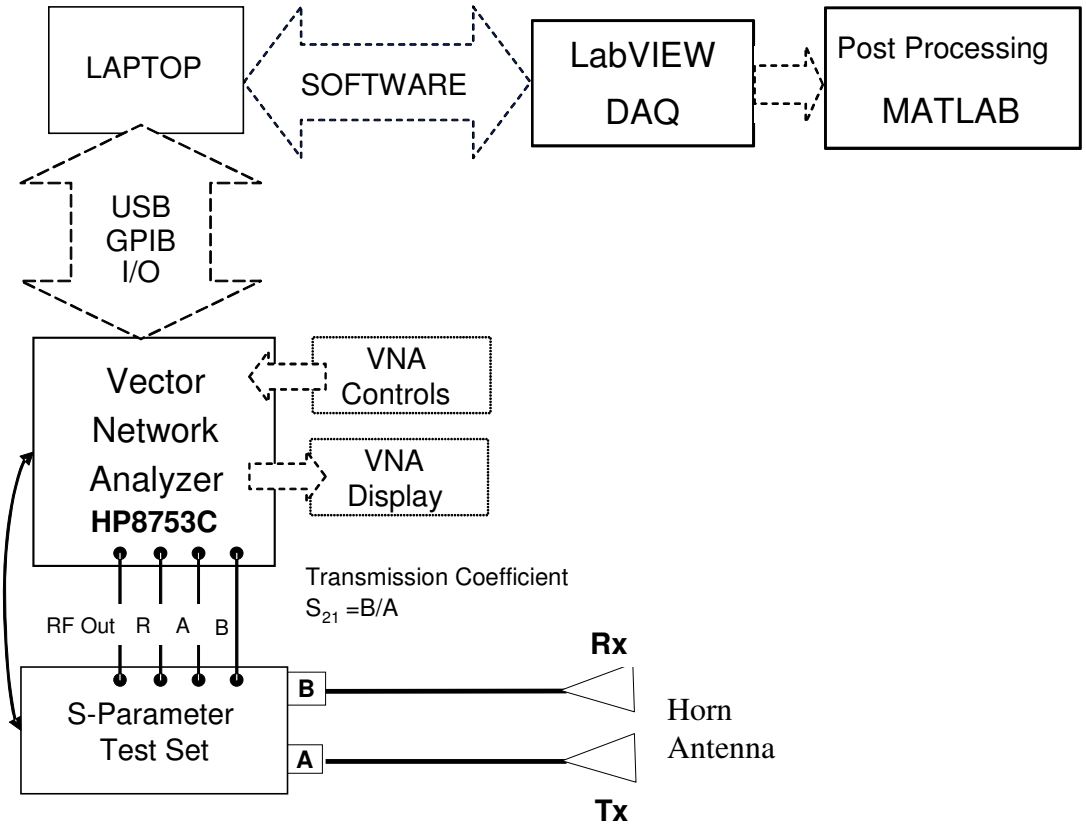

Figure 4.1: Measurement System

Network analyzers measure the reflection and transmission characteristics of devices and networks by applying a known frequency swept signal; and measuring the

reflected signal. The signal transmitted through the device or reflected from its input is compared with the incident signal generated by a swept RF source. The signals are applied to a receiver for measurement, signal processing and display. A network analyzer consists of a source, signal separation devices, a receiver, and a display. The HP8753C vector network analyzer integrates a high resolution synthesized RF source and a dual channel three-input receiver to measure and display magnitude, phase, and a group delay of transmitted and reflected power. [14]

Figure 4.2: HP8753C Vector Network Analyzer

The signal from the HP8753C Vector Network Analyzer must be captured for processing. A GPIB-USB data acquisition (DAQ) interface is used to acquire the data into the computer. The virtual instrumentation software NI-LabVIEW, a graphical

programming platform is used to create user-defined DAQ system. [10] LabVIEW platform provides specific tools and models to solve specific applications ranging from modular measurement to hardware control.

Due to finite dynamic range, isolation and directivity characteristics we need to perform vector accuracy enhancement, known as measurement calibration or error correction, provides the means to simulate a perfect measurement system. High frequency measurement there are measurement errors associated with the system that contribute to uncertainty in the results. Parts of the interconnecting cables and signal separation devices along with the analyzer introduce magnitude and phase variations. These variations appear as superposition of erroneous signals on the measured data. The VNA measurement calibration procedure measures magnitude and phase responses from known standard devices, and compares the measurement with actual device data. It uses the results to characterize the system and effectively remove the system errors using vector math capabilities internal to the network analyzer from the measurement data [13].

`

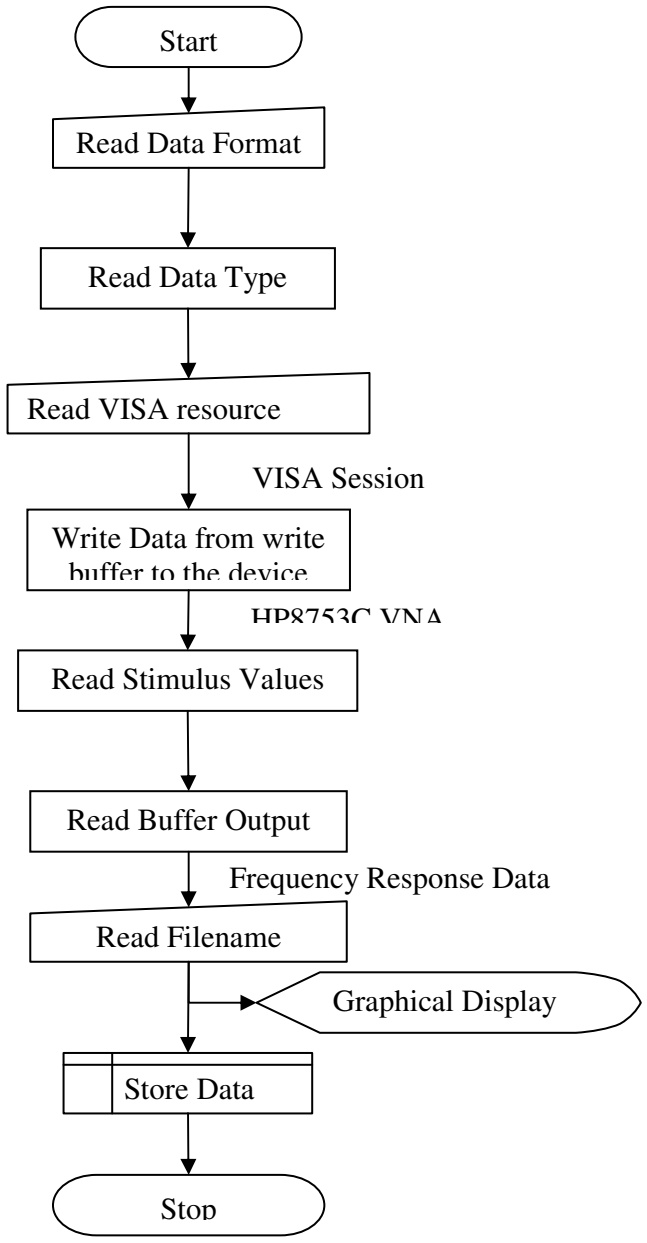

Figure 4.3: Measurement Flow Diagram

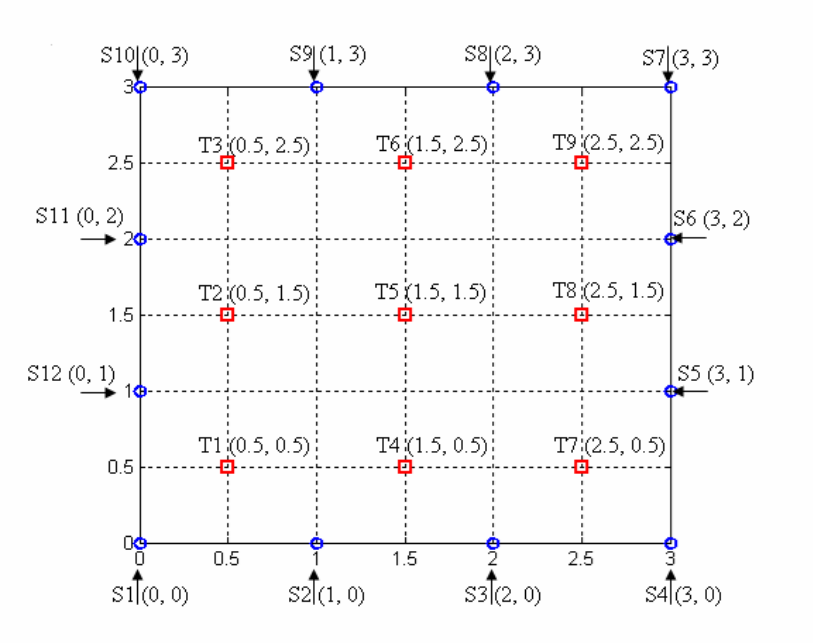

Figure 4.4: Experimental localization geometry

The radar sensor transmits sequences of sinusoidal signals of different frequencies toward a target, receives return signals from the target, and processes them for extracting the target characteristics. A Styrofoam is used as the dielectric medium to support the target. The typical experimental setup is shown above. The transmitted radar signal is converted into a reflected signal due to the electromagnetic scattering from a target. For the experimental study, we are using the monostatic mode of operation. Hence, even though the target scatters the incident radar energy in all directions, only the fraction of energy scattered back to the radar receiver is of interest. This is referred to as the back scattered energy.

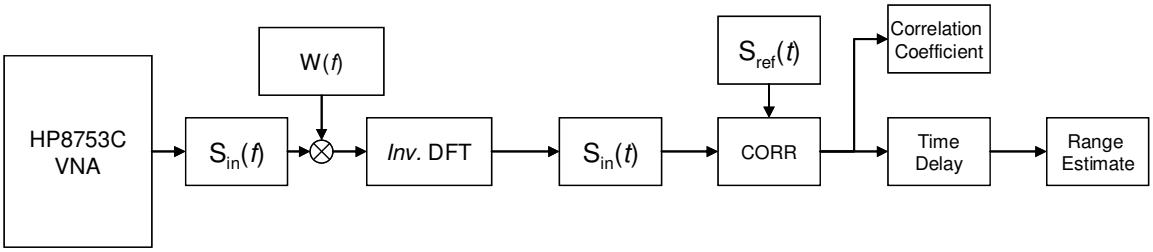

Figure 4.5: Experimental Flow diagram

The transmitted wave is given by the equation as given below.

$$T_R(t) = \sum_n A_n e^{j2\pi f_n t} \qquad (4.1)$$

The back scattering equation form a point scatterer model is given by the equation below [26].

$$S_R(t) = \sum_n A_n e^{j2\pi f_n (t - t_{i_n})} \qquad (4.2)$$

$$S_R(t) = \sum_n A_n e^{j2\pi f_n (t - \frac{2R_n}{c})} \qquad (4.3)$$

Where A_n represents the strength of the nth scattering center and R_n represents its location along the radar line of sight (down range direction). Clearly if the signal is a narrow pulse, then based on the point-scatterer model the reflected signal is comprised of a collection of pulses where the pulse locations indicate the spatial positions of the scattering centers on the target along the down range and direction and the strengths of

the scattering centers are proportional to the strengths of the scattering centers and the distance of the scattering center form the antenna.

Figure 4.6: Experimental Setup

The data obtained from the HP875C Vector Network Analyzer is in the frequency domain. The frequency range is set to 1GHz to 3GHz. The frequency range is divided into 201 Frequency samples. The power is set to +15 dBm. The averaging factor is set to 16 samples. The HP8753c Vector Network Analyzer is calibrated using the 2-port reflection, VNA calibration routine to estimate and compensate for the discontinuities due to the cable interfaces and long coaxial cables used to connect the

antennas. Based on the geometrical theory of diffraction (GTD), derived on the electromagnetic fields in the frequency domain $\omega = 2\pi f$.

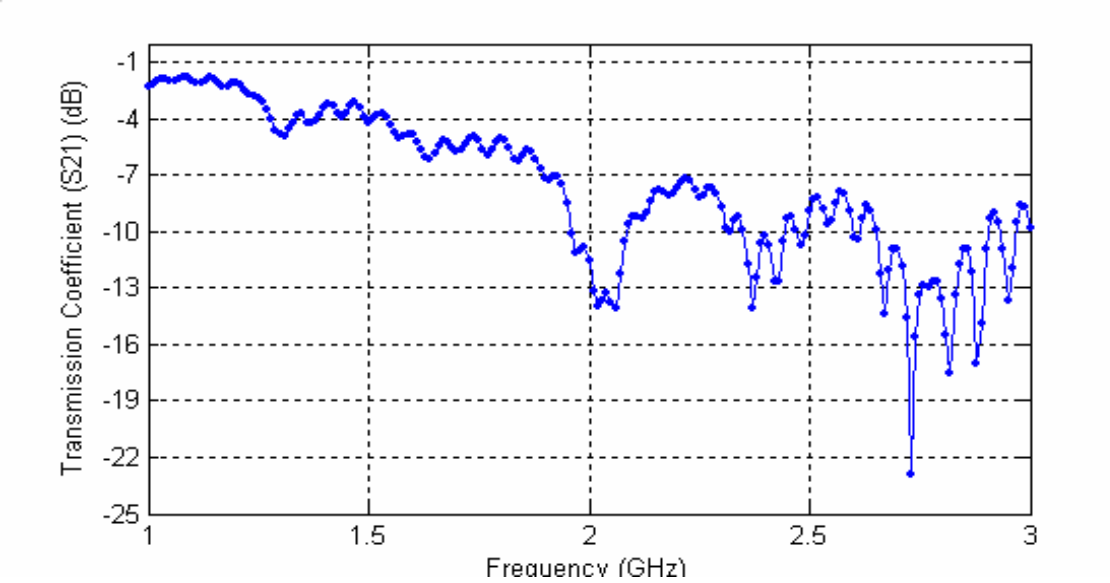

Figure 4.7: Transmission Coefficient (S_{21}) measured in the Frequency Domain

The transmission coefficient (S_{21}), measured by the VNA is given by

$$S_{21} = \frac{\sum_n r_n A_n e^{j2\pi f\left(t - t_{in}\right)}}{\sum_n A_n e^{j2\pi ft}} \qquad (4.4)$$

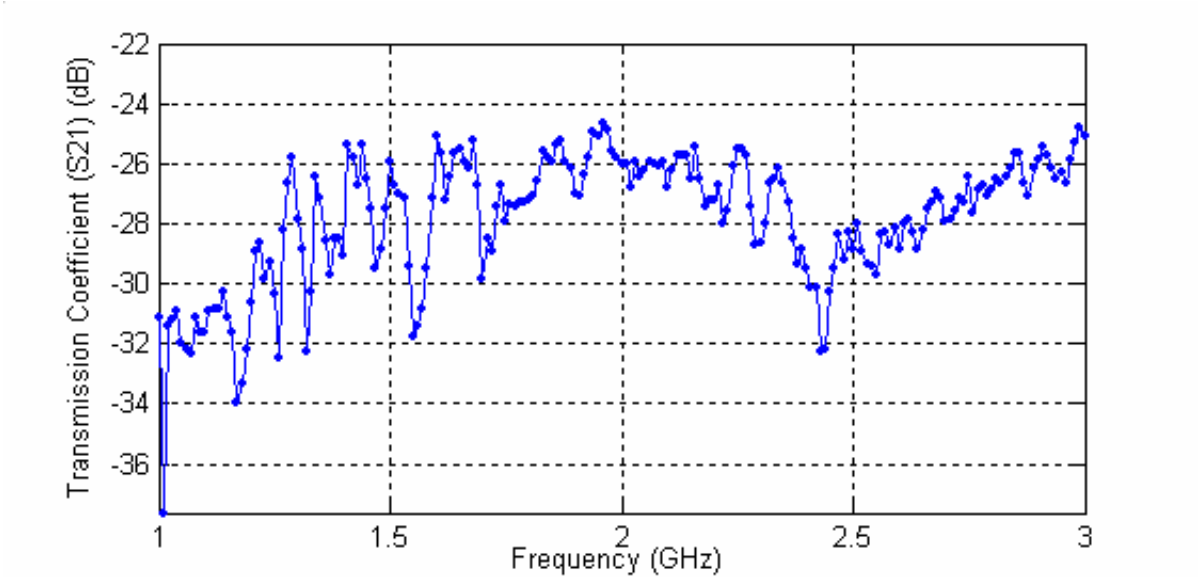

Figure 4.8: Frequency Domain Signal (Sin(f)) after Background Subtraction

The data obtained in the frequency domain *x*(*f*). The sampled signal values are multiplied by the Hanning function *w*(*f*) to reduce the time lobes. The Hanning window function is defined as follows:

$$w[k+1] = 0.5\left(1 - \cos\left(2\pi \frac{k}{n-1}\right)\right), k = 0,....,n-1 \qquad (4.5)$$

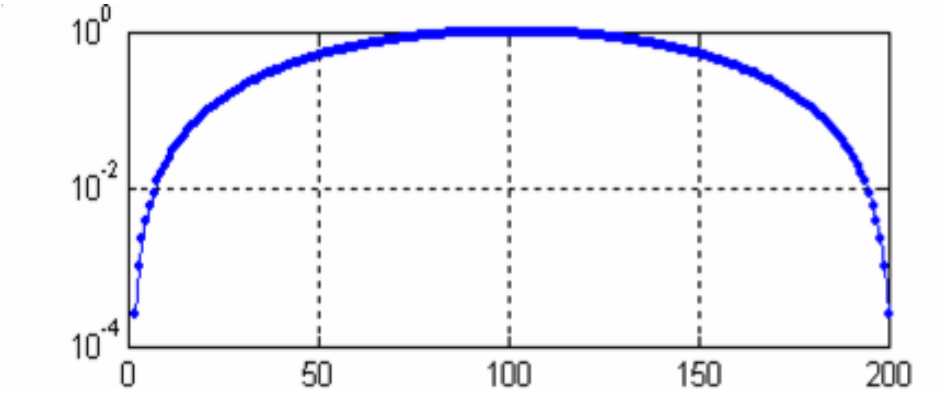

Figure 4.9: Hanning Window (W(f))

The resultant is then transformed into the time domain using the Inverse Discrete Fourier Transform

$$x(n) = \sum_{k=0}^{N-1} x(k) e^{jk2\pi/N} = 0,...., N-1 \qquad (4.6)$$

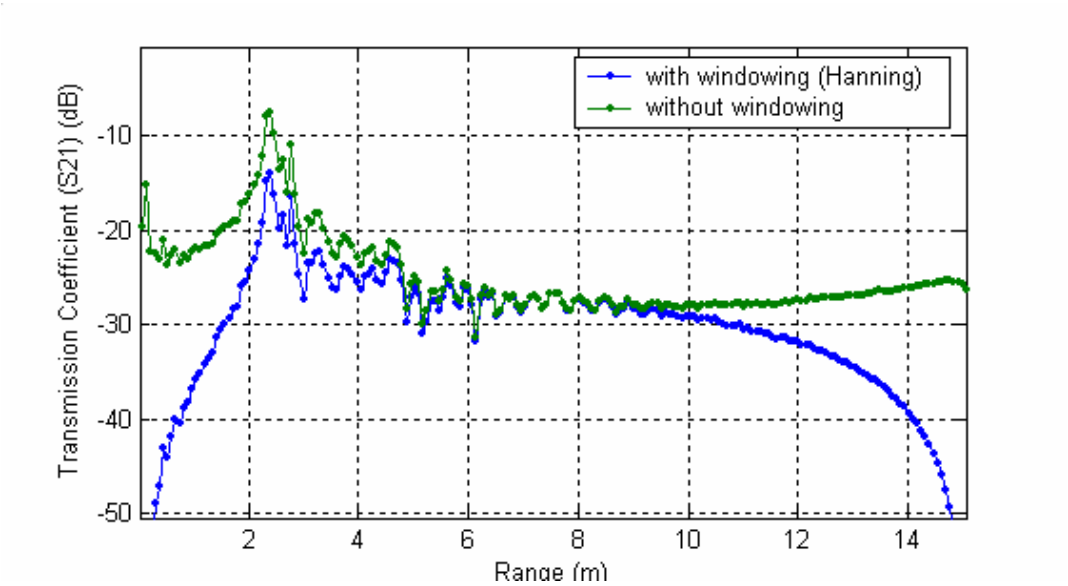

Figure 4.10: Time Domain Signal

The resultant signal is then correlated with the reference signal used as the correlation matched filter at the receiver. Correlation is carried out by computing the cross correlation of a stored reference waveform with the measured response of an unknown target. From the principles of noise radar [34], the simplest form of a noise radar transmits a random noise signal $S_{in}(t)$.

$$S_{corr} = \frac{1}{T-\tau}\int_{\tau}^{T} S_{ref}(t) S_{in}(t-\tau)dt \qquad (4.7)$$

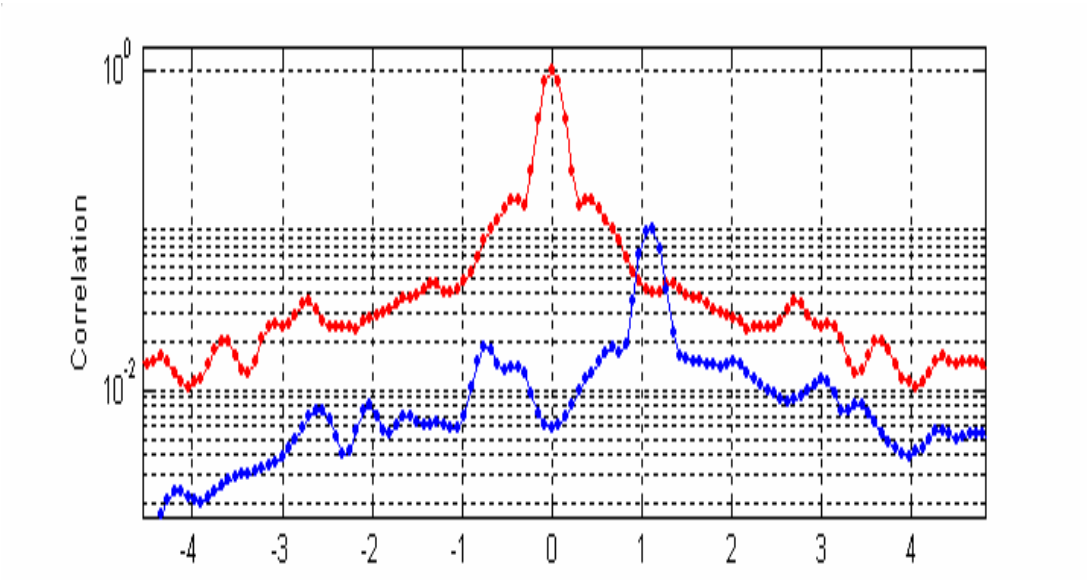

Figure 4.11: Range estimation using signal correlation

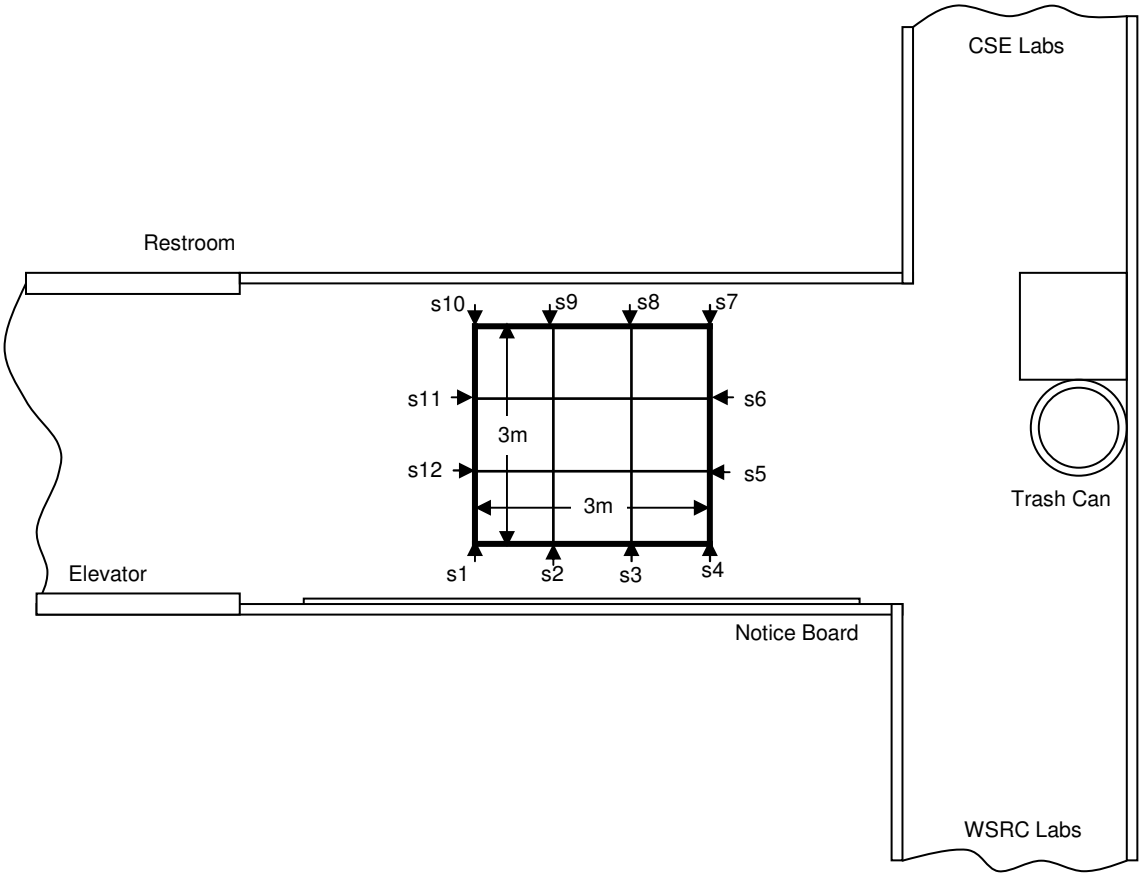

Figure 4.12: Floor map for the localization experiment

Figure 4.13: Radar measurements

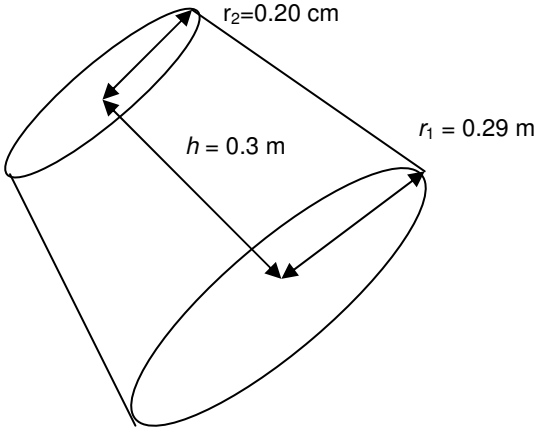

Figure 4.14: Target 1 Dimensions

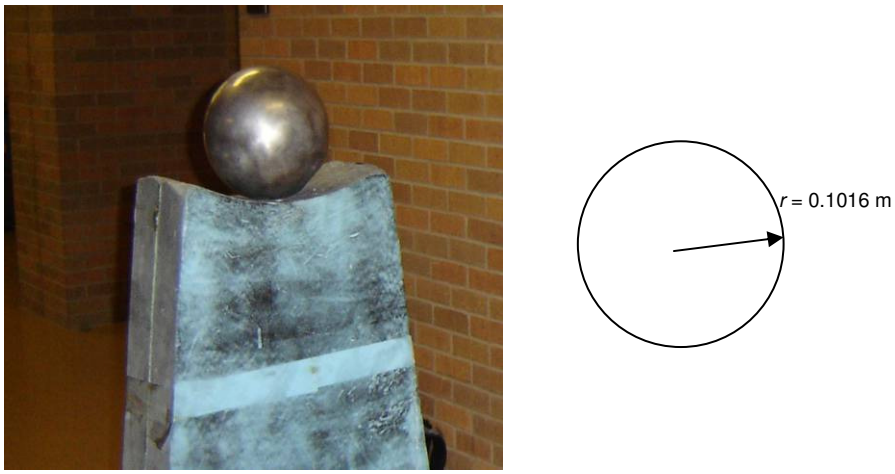

Figure 4.15: Target 2 Dimensions

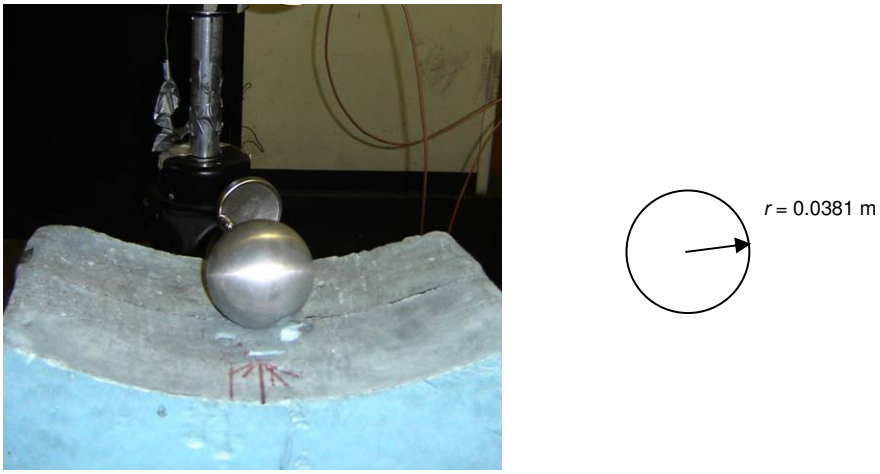

Figure 4.16: Target 3 Dimensions

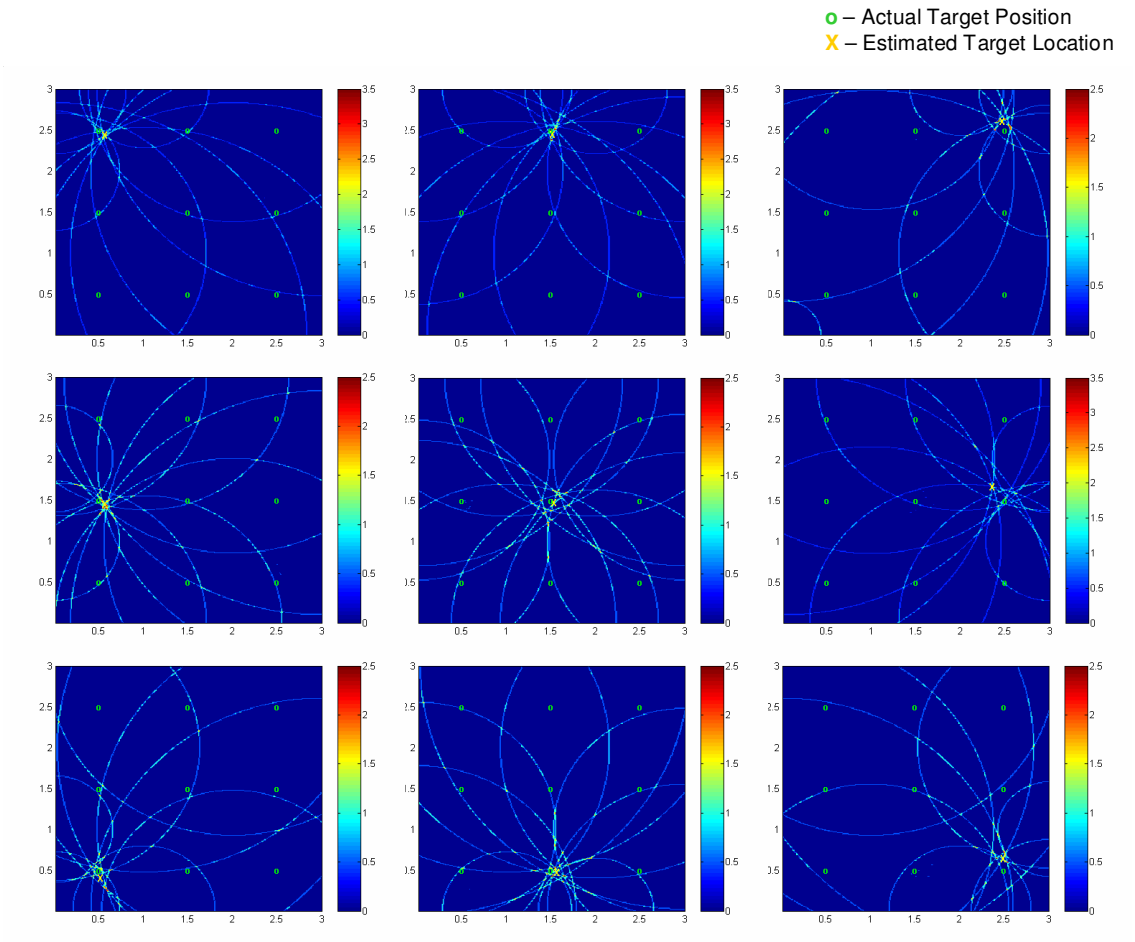

Figure 4.17: Hough Transform Inspired Algorithm – Target 1

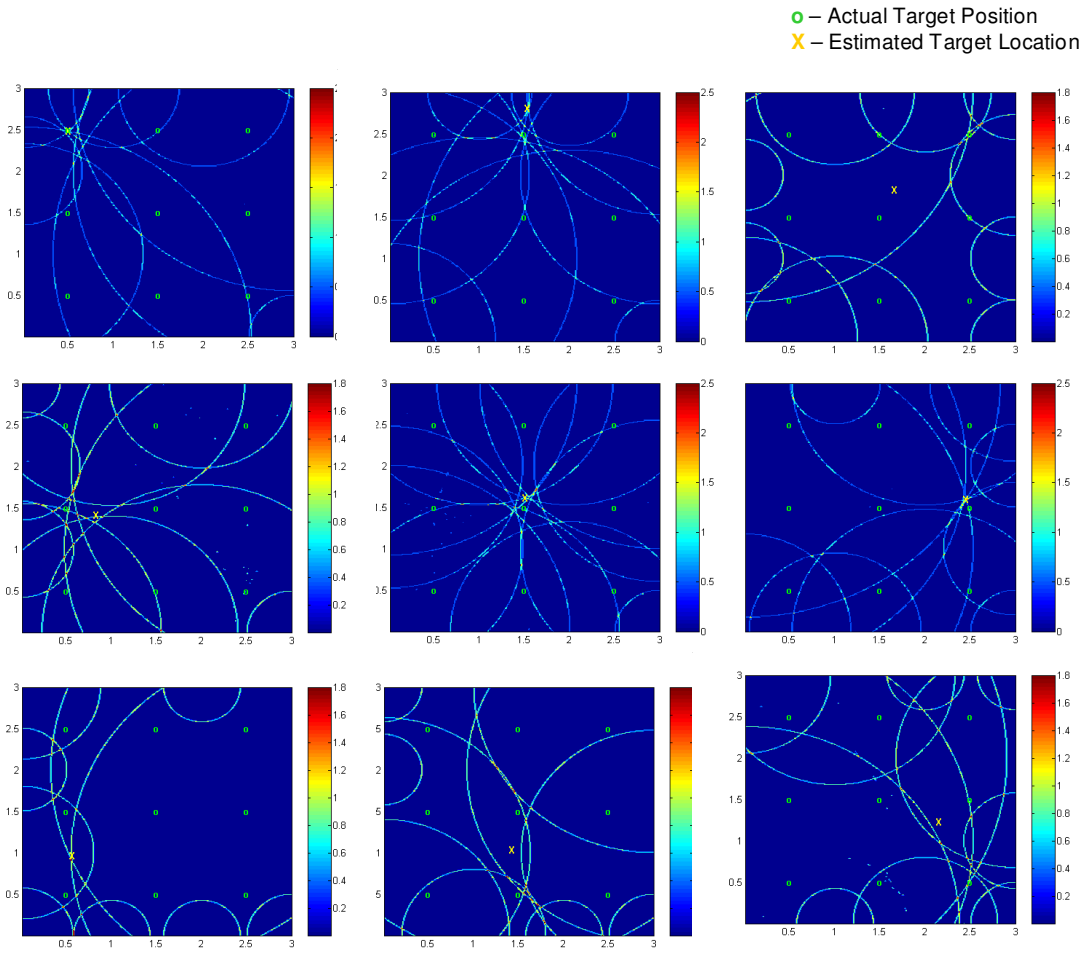

Figure 4.18: Hough Transform Inspired Algorithm – Target 2

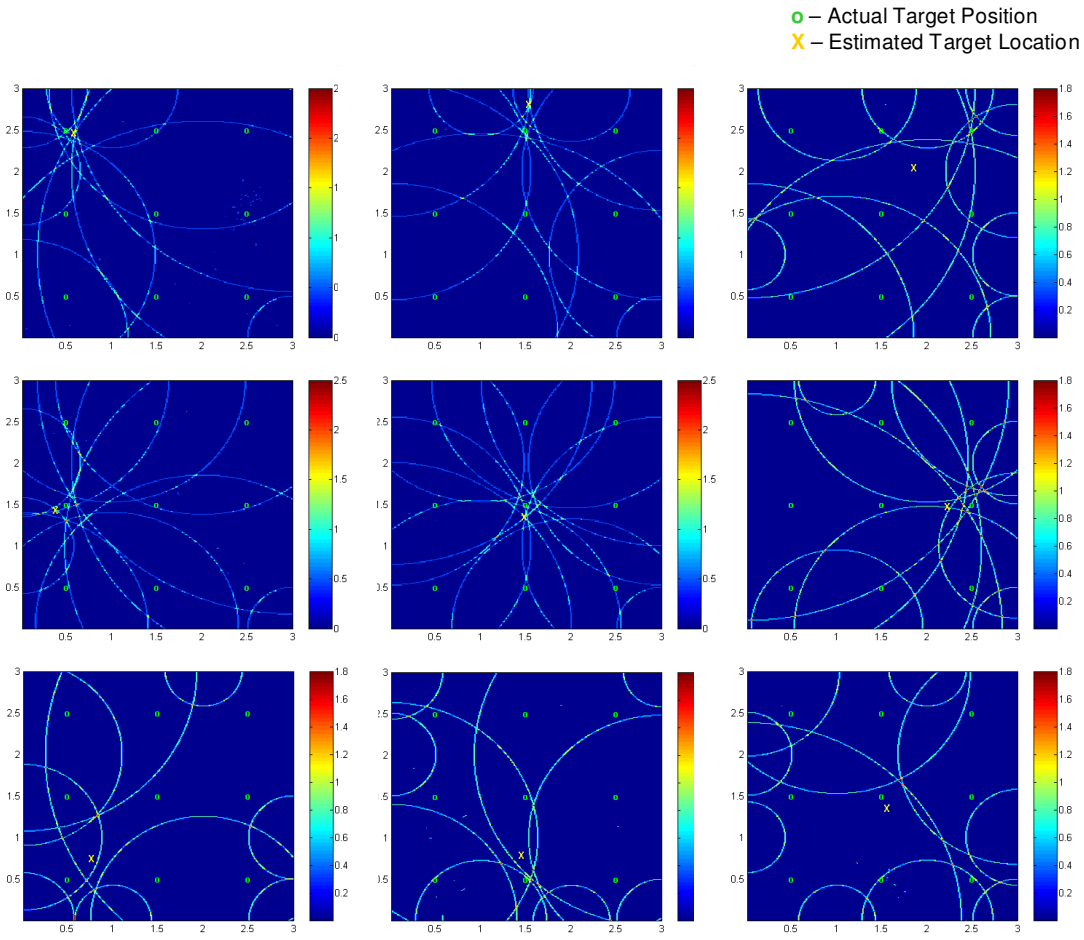

Figure 4.19: Hough Transform Inspired Algorithm – Target 3

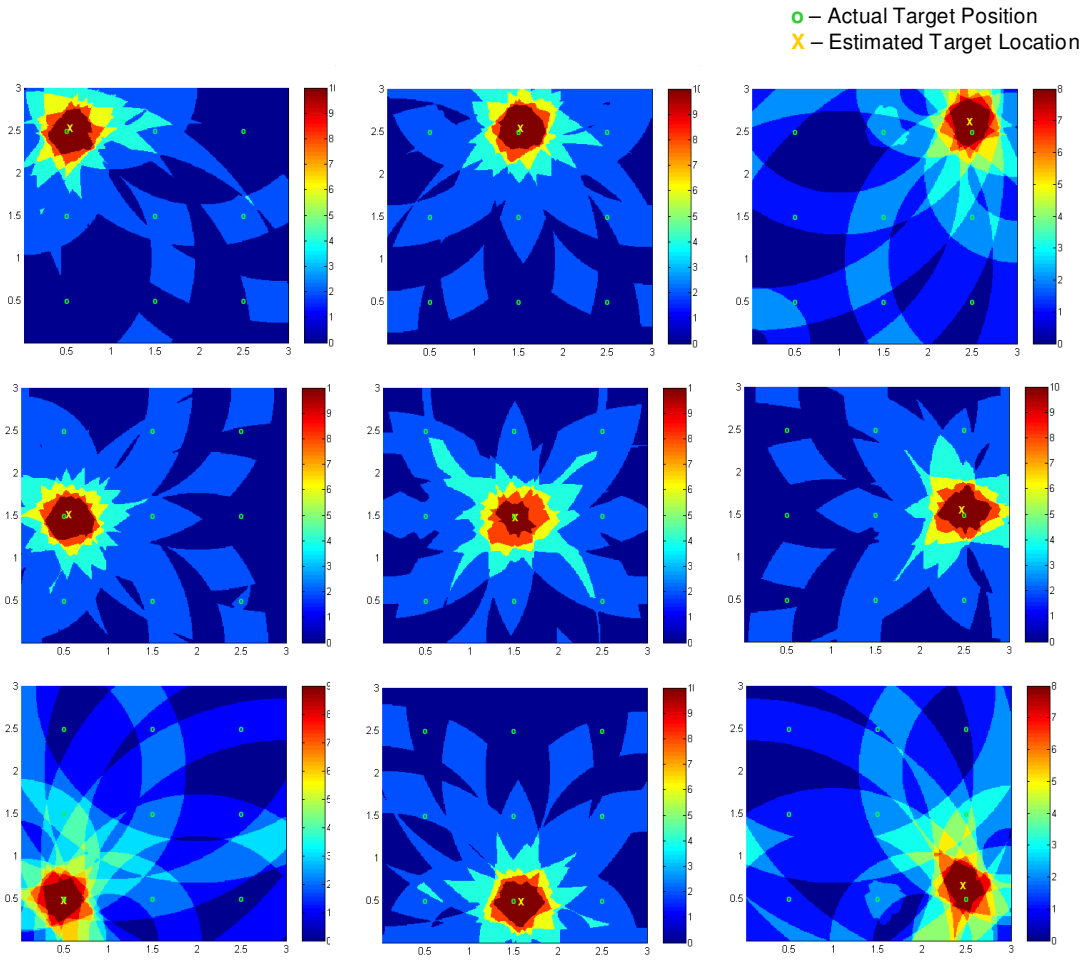

Figure 4.20: Voting based Algorithm – Target 1

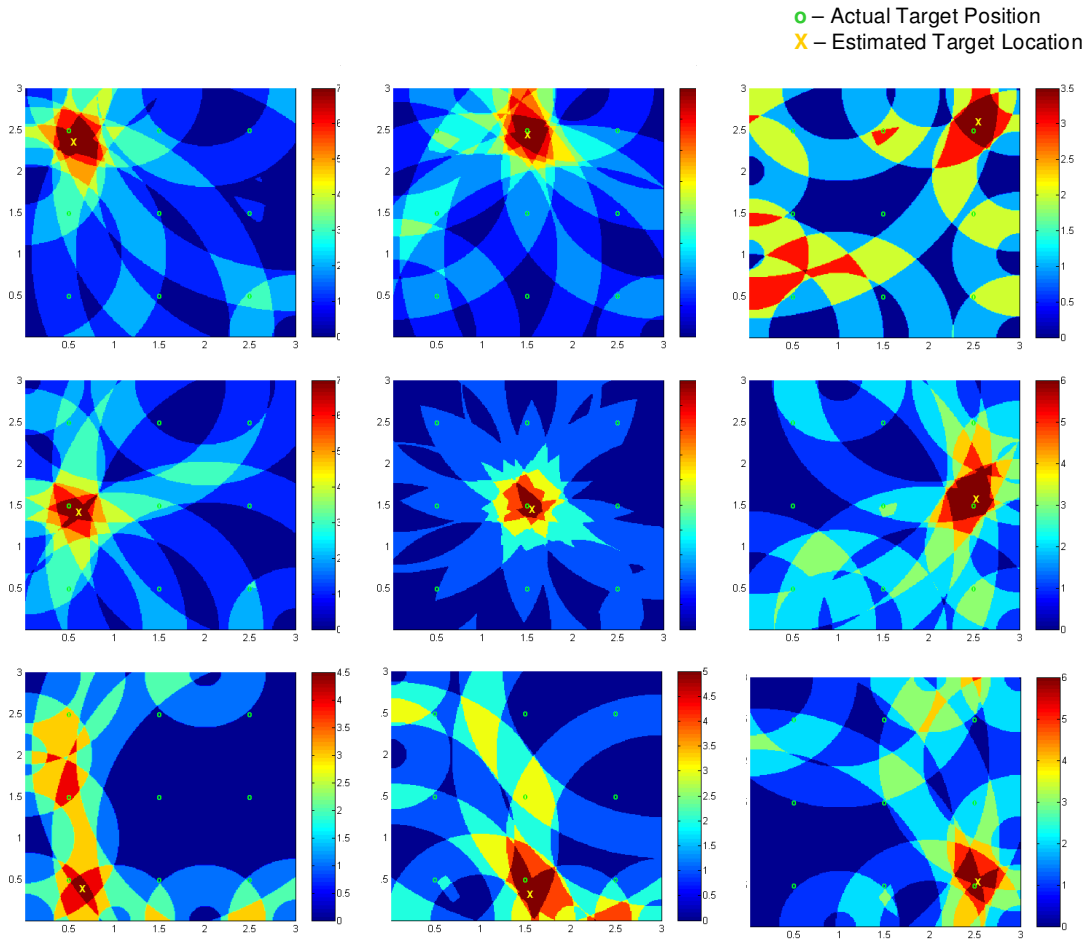

Figure 4.21: Voting based Algorithm – Target 2

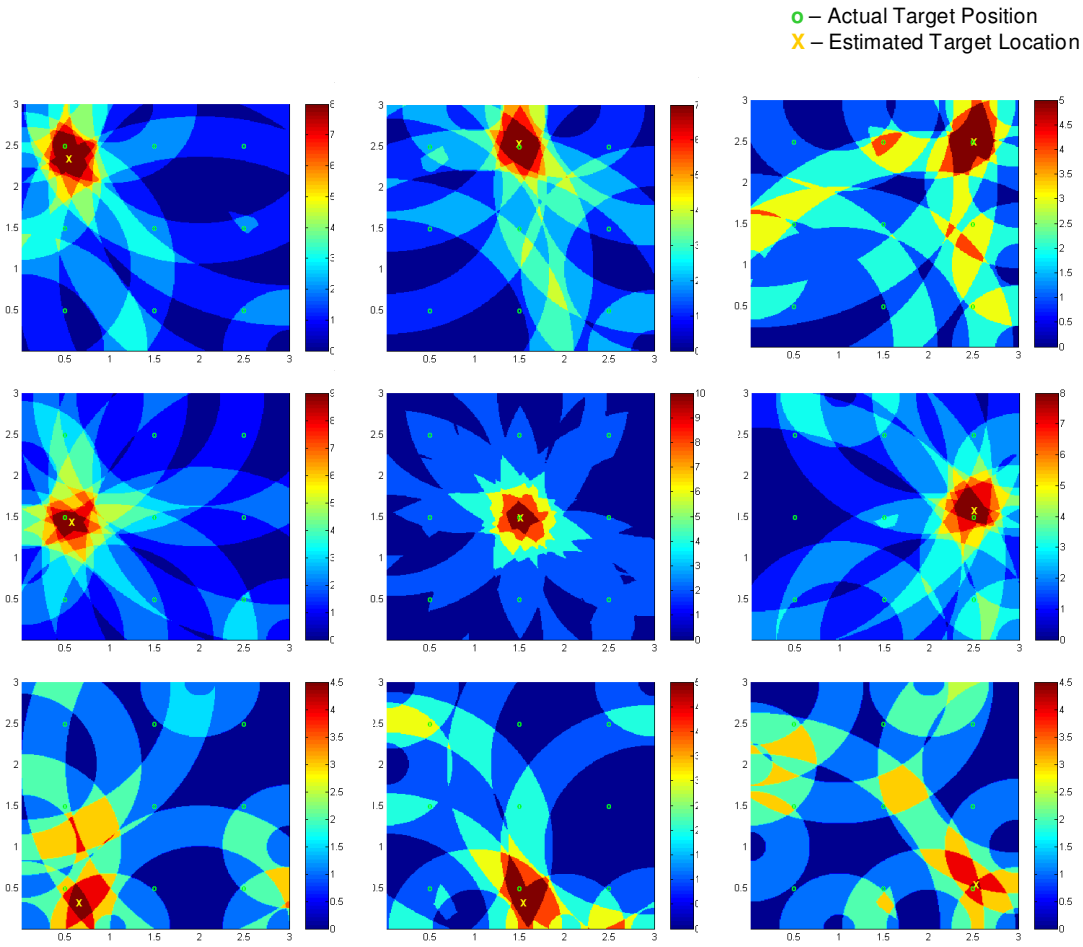

Figure 4.22: Voting based Algorithm – Target 3

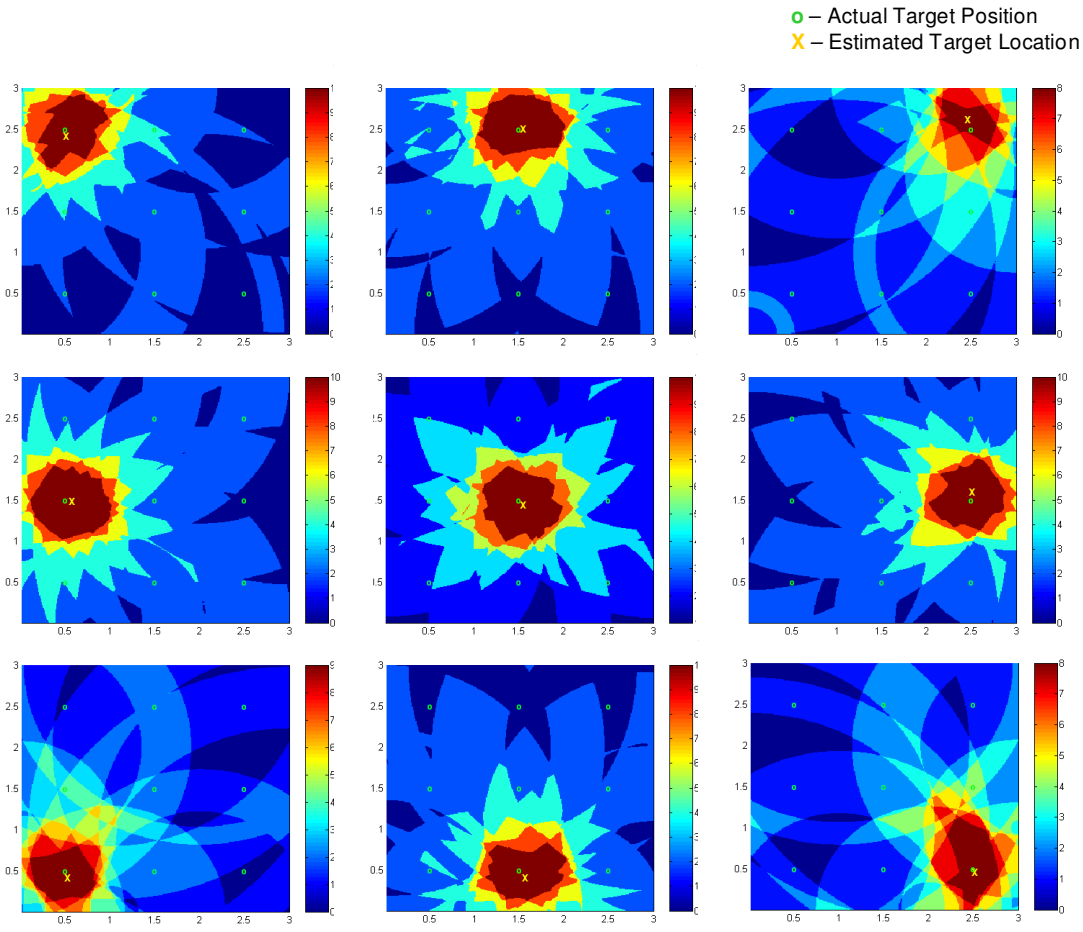

Figure 4.23: Modified – Grid Based Localization for Target T1

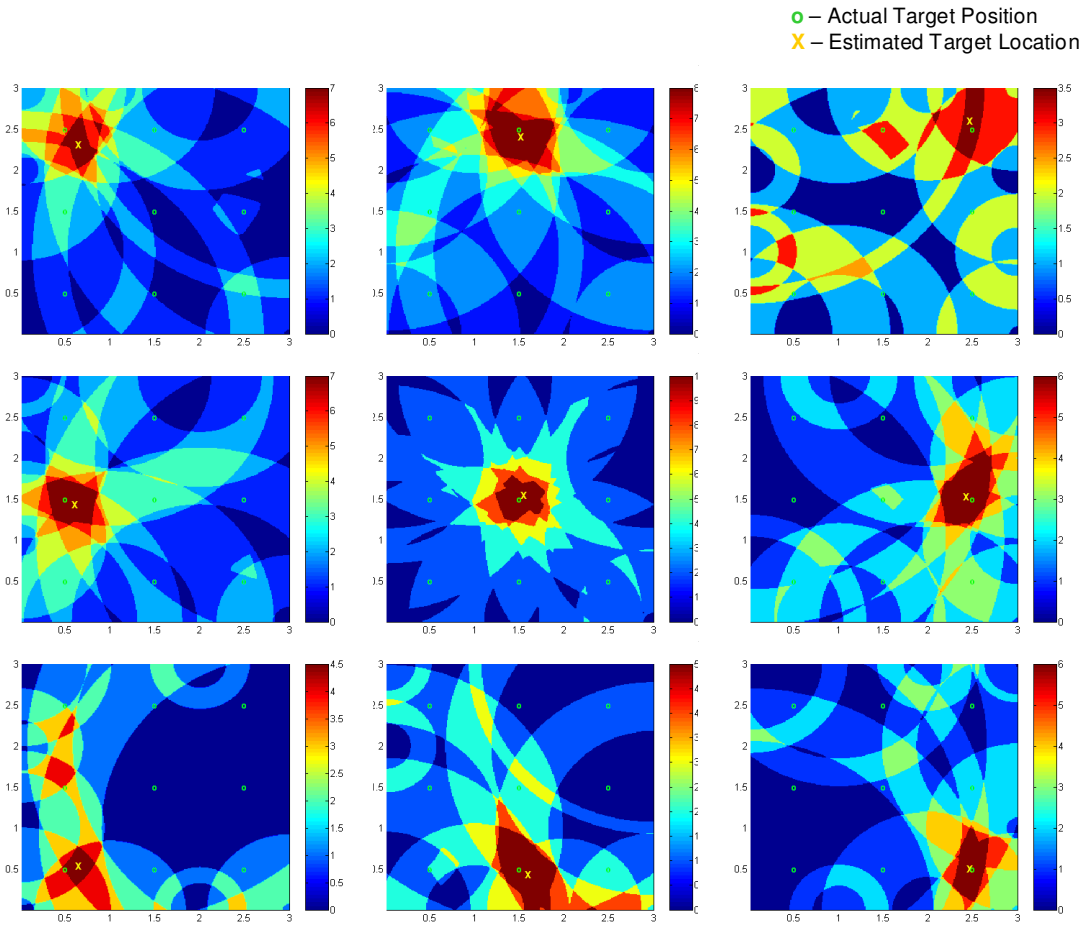

Figure 4.24: Modified – Grid Based Localization for Target T2

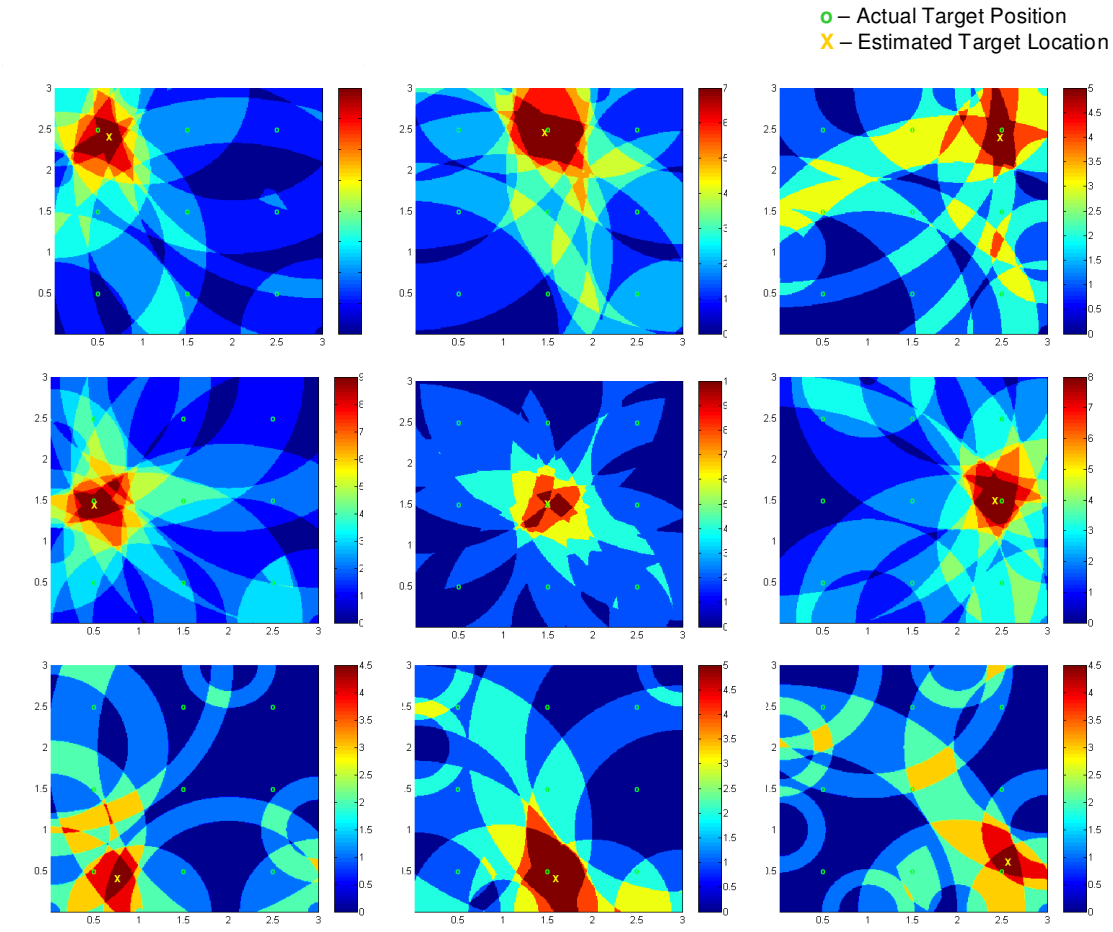

Figure 4.25: Modified – Grid Based Localization for Target T3

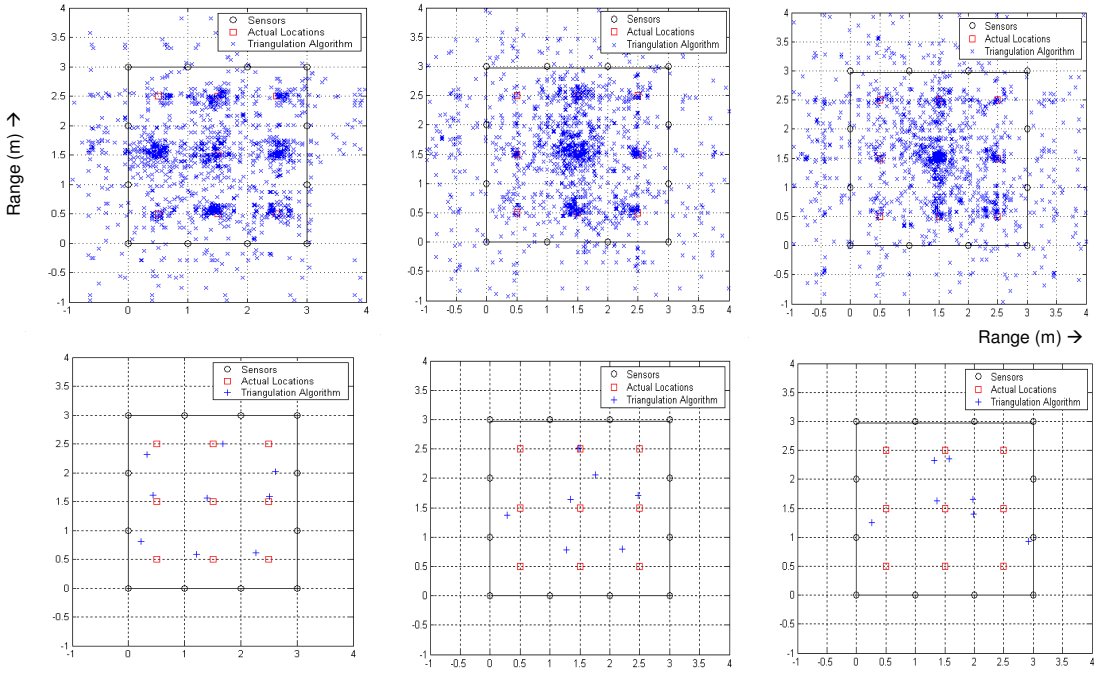

Figure 4.26: Localization using MMSE algorithm for Targets T1, T2, T3 (left - right)

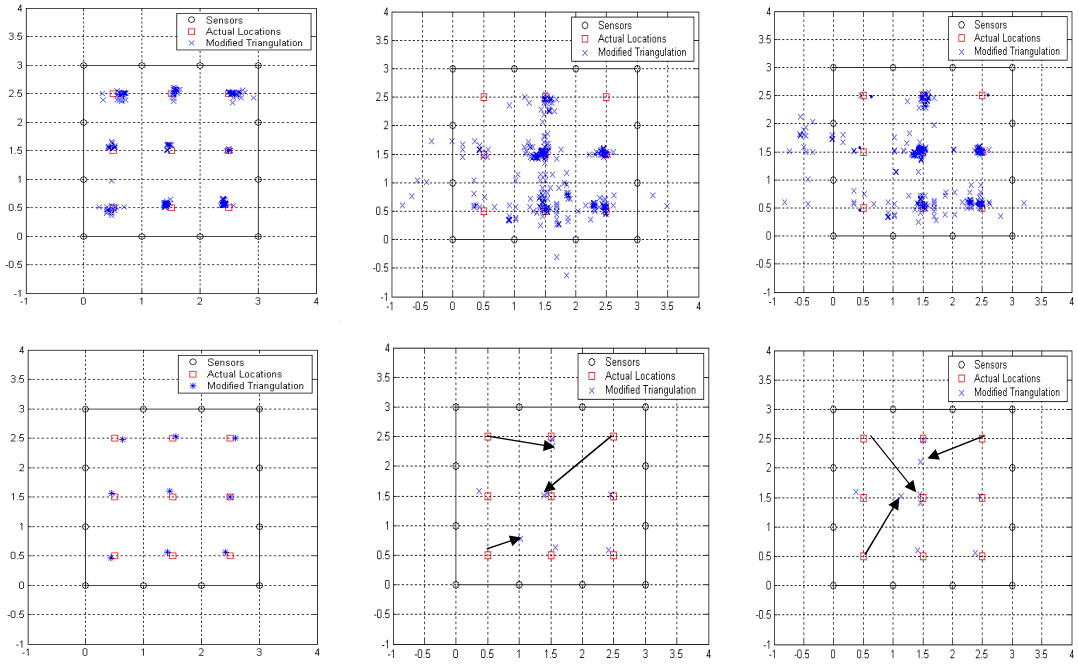

Figure 4.27: Localization using MMSE algorithm for Targets T1, T2, T3 (left - right)

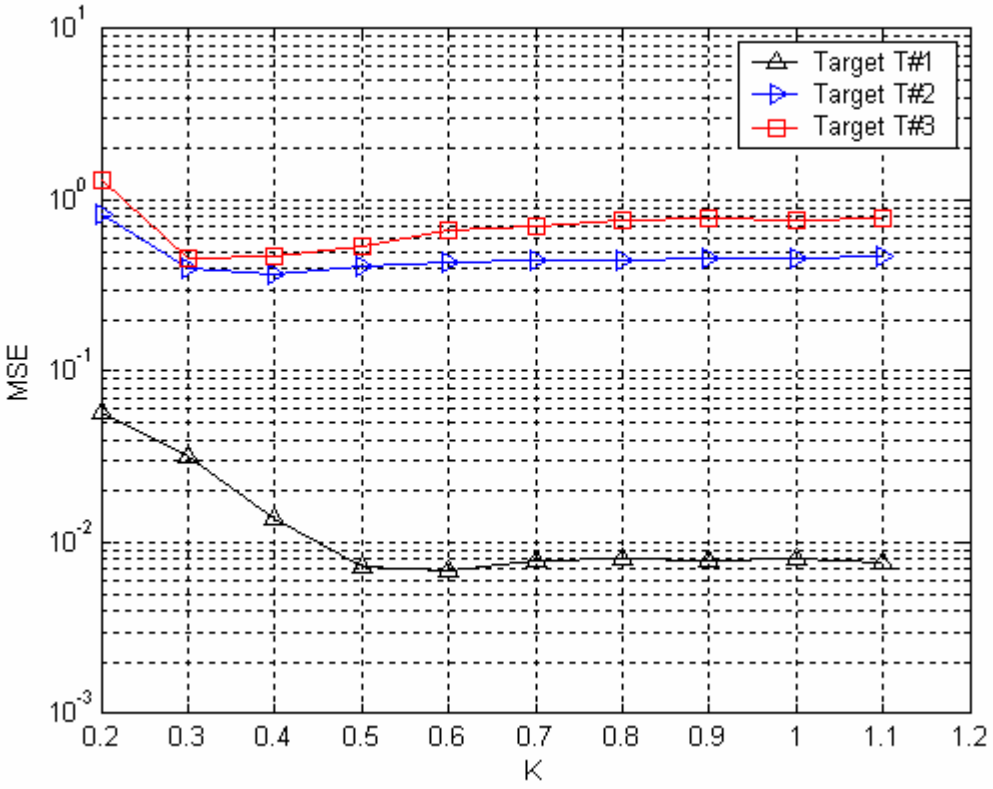

Figure 4.28: Effect of Variation of parameter γ2

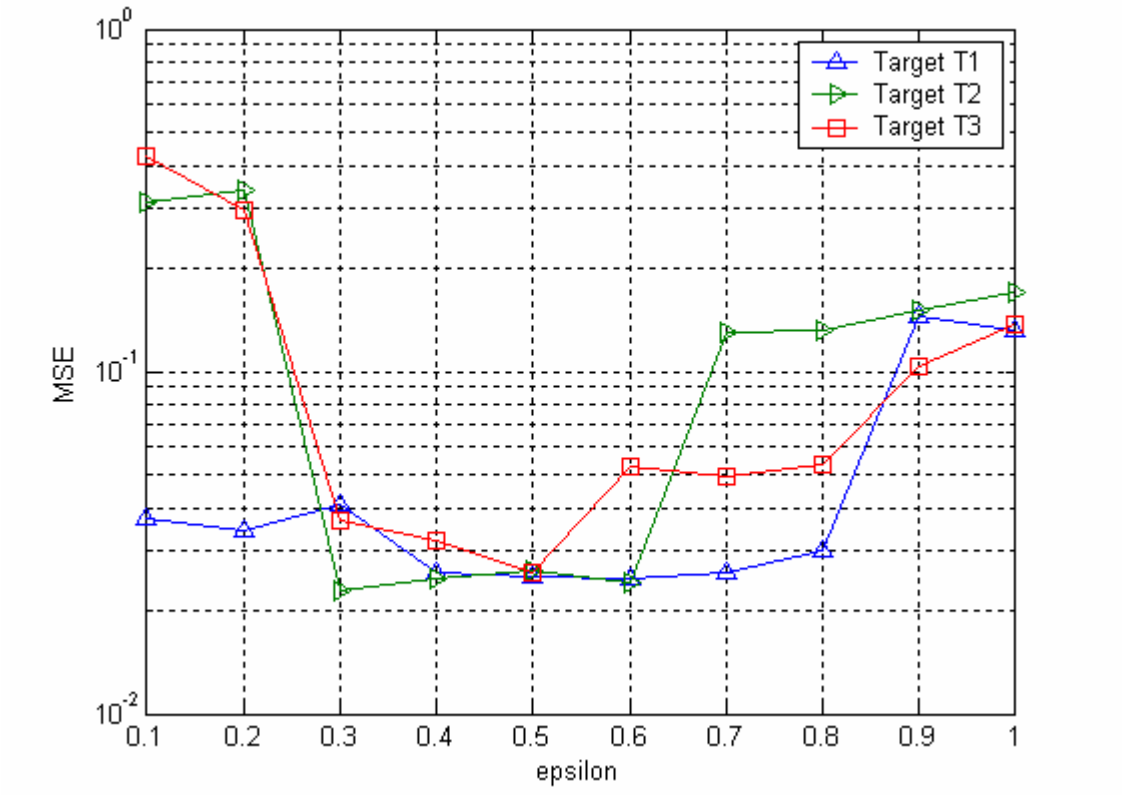

Figure 4.29: Effect of Variation of parameter Є

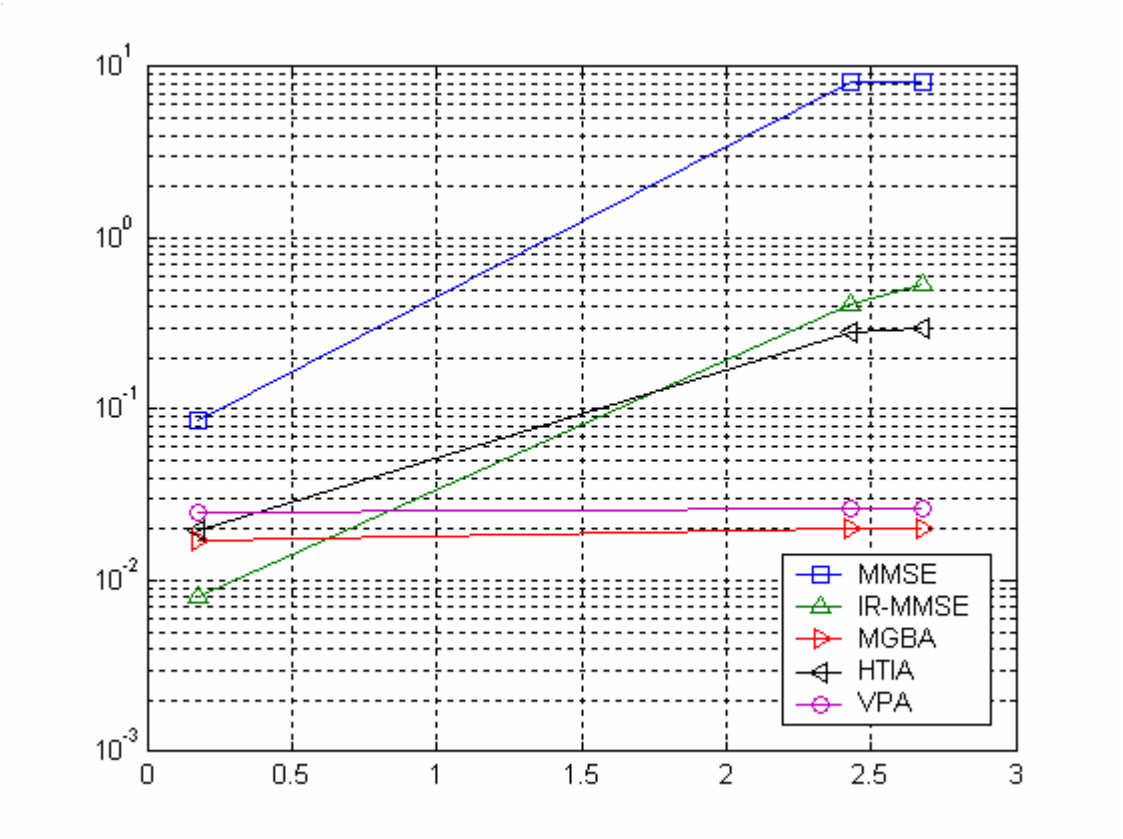

Figure 4.30 Performance Analysis

The performance comparison of the algorithms reveals that the grid based algorithms (MGBA, VPA, HTIA) out-perform the MMSE and IR-MMSE algorithms for large sensor range estimation errors. The robustness of the algorithms is reflected in the experimental results.

Table 4.1 A Comparison of Localization Algorithms

Algorithm / Target	Target 1	Target 2	Target 3
Range Estimation Mean Square Error	0.1779	2.2293	2.6751
Minimum Mean Square Error Estimation	0.0854	8.0648	8.2517
Iteratively Refined - Minimum Mean Square Error Estimation ($\gamma = 0.5$)	0.0080	0.4145	0.5447
Modified Grid Based Algorithm ($K = 1$)	0.0173	0.0199	0.0201
Hough Transform Inspired Algorithm	0.0195	0.2822	0.2948
Voting based Algorithm ($\epsilon = 0.5$)	0.0250	0.0262	0.0265

CHAPTER 5

CONCLUSIONS AND FUTURE WORK

In this work, we have proposed an improved algorithm for localization of passive targets in radar networks. The proposed Modified Grid Based Algorithm (MGBA) demonstrates better performance in presence of large range estimation errors. In this thesis, we have provided both - numerical approach and experimental validation of the proposed algorithm. In the multiple targets scenario, the degree of complexity increases multifold since the number of targets is itself a variable. Additional complication is introduced due to multiple reflections bouncing from the targets. The time domain signal is a summation of the scattered field and the target interactions. The time domain signal may be resolved into the individual targets using targets' radar signature and pattern recognition. The problem is now reduced to single target localization for each target considered individually. However, the Grid – Based Graphical approaches is applicable to simultaneous localization multiple targets scenario. A simulation study by Chang *et al.*[4] using the HTIA illustrates the application of the algorithm for simultaneous localization of multiple targets in the MSSO (Multiple Sensor Multiple Object) case analysis.

APPENDIX A

MMSE LOCALIZATION ALGORITHM

Inputs: Anchor locations and range estimates (x_{si}, y_{si}, d_{si})

Output: Target Position (x, y)

---

1. Estimate matrix A based on (x_{si}, y_{si}, d_{si})

$$A = \begin{bmatrix} (x_1 - x_2)^2 & (y_1 - y_2)^2 \\ \vdots & \vdots \\ (x_1 - x_n)^2 & (y_1 - y_n)^2 \end{bmatrix}$$

2. Estimate column matrix u

$$u = \begin{bmatrix} x \\ y \end{bmatrix}$$

3. Estimate the target position using Least Squares Estimate

$$u = (A^T A)^{-1} A^T b$$

APPENDIX B

IR-MMSE LOCALIZATION ALGORITHM

Inputs: Anchor locations and range estimates (x_{si}, y_{si}, d_{si})

Output: Target Position (x, y)

---

1. Estimate matrix A based on (x_{si}, y_{si}, d_{si})

$$A = \begin{bmatrix} (x_1 - x_2)^2 & (y_1 - y_2)^2 \\ \vdots & \vdots \\ (x_1 - x_n)^2 & (y_1 - y_n)^2 \end{bmatrix}$$

2. Estimate column matrix u

$$u = \begin{bmatrix} x \\ y \end{bmatrix}$$

3. For all combinations of A_4 and b_4 (A_4 and $b_4$are any four rows of A and b)

$$u = A_4^{-1} b_4$$

4. Estimate ζ^2 for each target position estimate (x_o, y_o) using A_4, b_4

$$\zeta^2 = \sum_{i=1}^{m} \left(d_i - \sqrt{(x_o - x_i)^2 + (y_o - y_i)^2} \right) \leq \gamma^2$$

Threshold γ^2 is a tunable parameter depends on the measurement error model

5. Eliminate target position estimate (x_o, y_o) which do not satisfy criteria 4

6. Repeat step 4 until all target position estimates (x_{oi}, y_{oi}) for all i

7. Estimate the updated Target Position Estimate as (mean x_{oi}, mean y_{oi})

APPENDIX C

HOUGH TRANSFORM INSPIRED ALGORITHM

Inputs: Anchor locations and range estimates (x_{si}, y_{si}, d_{si})

Output: Target Position (x, y)

---

1. Discredited the square region of interest into N x N grids.
2. Search on all the grid-points for local maximal points of score function S(x; y), generate a candidate set f(x_i; y_i); $i = 1 \ldots K$, .
3. For the grid point (x_i, y_i), where (x_i; y_i) > γ, report a discovery of the target.

APPENDIX D

VOTING BASED ALGORITHM “VOTING PROCESS”

Inputs: Anchor locations and range estimates (x_{si}, y_{si}, $d_{si, \epsilon}$)

Output: Target Position (x, y)

---

1. G_m, $S(x, y) = [\ ]$; $(x, y) \in G_m$

$$G_m = \begin{bmatrix} 0 & 0 & 0 & 0 \\ \vdots & \ddots & & \vdots \\ \vdots & & \ddots & \vdots \\ 0 & 0 & 0 & 0 \end{bmatrix}$$

2. Serially scan each grid and determine score function

   if $d_i^l \le \sqrt{(x_i - x)^2 + (y_i - y)^2} \le d_i^u$

   then $s(x, y) = s(x, y) + w_k$

   endif

3. Maximize Score Function S(x, y)

4. Estimate the Target Position (x, y) as the centroid of Max[S(x; y)]

APPENDIX E

MODIFIED GRID BASED ALGORITHM

Inputs: Anchor locations and range estimates (x_{si}, y_{si}, d_{si})

Output: Target Position (x, y)

---

1. G_m, $S(x, y) = [\ ]$; $(x, y) \in G_m$
2. Determine $\varepsilon = S_{corr}$
3. Serially scan each grid and determine score function

   if $d_i^l \le \sqrt{(x_i - x)^2 + (y_i - y)^2} \le d_i^u$

   then $s(x, y) = s(x, y) + w_k$

   endif
4. Maximize Score Function S(x, y)
5. Estimate the Target Position (x, y) as the centroid of Max[S(x; y)]

APPENDIX F

CENTROID FUNCTION

Inputs: Image (Im), Threshold (γ)

Output: Centroid (x_c, y_c)

---

[1] Convert the image Im (x, y) into a binary image

If Im (x_i, y_i) $\geq \gamma$

then Im (x_i, y_i) = 1

else

Im (x_i, y_i) = 0

endif

[2] Compute Area of Image $area = \sum_x \sum_y \mathrm{Im}(x, y)$

[3] Define size of Image [rows, cols] = size (Im)

[4] Define matrices x_g and y_g as follows

$$x_g = \mathrm{ones}(\mathrm{rows},1) * [1 : \mathrm{cols}] \quad x_g = \begin{bmatrix} 1 & 2 & 3 & \cdots & rows \\ 1 & 2 & 3 & \cdots & rows \\ & & & \ddots & \\ 1 & 2 & 3 & \cdots & rows \end{bmatrix}$$

$$y_g = [1:\text{rows}]'*\text{ones}(1,\text{cols}) \quad x_g = \begin{bmatrix} 1 & 1 & 1 & \cdots & 1 \\ 2 & 2 & 2 & \cdots & 2 \\ & & & \ddots & \\ & & & & \\ cols & cols & cols & \cdots & cols \end{bmatrix}$$

[5] $$x_c = \sum_x \sum_y \text{Im}(x,y).x_g \Big/ \sum_x \sum_y \text{Im}(x,y)$$

and

$$y_c = \sum_x \sum_y \text{Im}(x,y).y_g \Big/ \sum_x \sum_y \text{Im}(x,y)$$

REFERENCES

[1] F. Akyildiz, W. Su, Y. Sankarasubramaniam, and E. Cayirci. “Wireless sensor Networks: A Survey”, Computer Networks, 2002.

[2] Nasipuri and K. Li. “A directionality based location discovery scheme for wireless sensor networks”, WSNA, 2002.

[3] F. Akyildiz, W. Su, Y. Sankarasubramaniam, and E. Cayirci. “Wireless sensor Networks: A Survey”, Computer Networks, 2002.

[4] Nasipuri and K. Li. “A directionality based location discovery scheme for wireless sensor networks”, WSNA, 2002.

[5] Savvides, C. C. Han, and M. B. Strivastava. “Dynamic fine-grained localization in ad-hoc networks of sensors”. In Proc. of ACM MobiCom, July 2001.

[6] Chang, C., “Localization and Object-Tracking in an Ultrawideband Sensor Network”, Masters Thesis, 2005

[7] Chang, C., Sahai, A., "Object tracking in a 2D UWB sensor network," Asilomar Conference on Signals, Systems, and Computers, November 2004

[8] Forsyth, D. A., Ponce, J., “Computer Vision – A Modern Approach”, Prentice Hall 2003

[9] Liu, D., Ning, P., Du, W., “Attack-resistant location estimation in sensor networks”, 2004

[10] Fretzagias and M. Papadopouli. Cooperative Location-Sensing for Wireless Networks. In Second IEEE International conference on Pervasive Computing and Communications, 2004.

[11] He, T., Huang, C., Blum, B. M., Stankovic, J. A., Abdelzaher, T. "Range-Free Localization Schemes for Large Scale Sensor Networks"

[12] National Instruments LabVIEW-8 Campus Workshop, http://www.ni.com/support/lvsupp.htm, 2006.

[13] National Instruments - LabVIEW Help document (Product Reference) , http://sine.ni.com/manuals/main/p/sn/n18:c,n23:4.28,

[14] John Paden, "Network Analyzer Operation", ITTC Summer Lecture Series, 2004

[15] Paden, J., "Network Analyzer Operation", ITTC Summer Lecture Series, Information and Telecommunication Technology Center, University of Kansas, 2004

[16] Agilent 8753C Network Analyzer Reference, 1989

[17] Bryant, G. H., "Principles of microwave measurement", London, Peregnnur, 1990.

[18] HP85033D, "User's and Service Guide", Agilent Technologies 3.5 mm Calibration Kit

[19] Cumming, I. G., Wong, F. H., Digital Processing of Synthetic Aperture Radar Data – Algorithms and Implementation, Artech house Inc. 2005

[20] Soumekh, M., "Synthetic Aperture Radar Signal Processing with MATLAB Algorithms", John Wiley & Sons, Inc. 1999

[21] Nirupama Bulusu, John Heidemann, Deborah Estrin, "GPS-less Low Cost Outdoor Localization for Very Small Devices"

[22] Tufan Coskun Karalar, Jan M. Rabaey, Implementation of a Localization System for Sensor Networks, PhD. Thesis 2006

[23] Dragos¸ Niculescu and Badri Nath, "Ad Hoc Positioning System (APS) Using AOA", DATAMAN Lab, 2003

[24] Aysegul Dersan, "Passive Target Localization by Time Difference of Arrival", 2002

[25] Bassem R. Mahafza and Atef Z. Elsherbeni, "MATLAB Simulations for Radar System Design", Chapman & Hall, 2004

[26] Brian Jersak, "Time Domian Analysis of Measured Frequency Domain Data", Masters Thesis 1988.

[27] Doug Rytting, "RF and Microwave Measurement Symposium and Exhibition - Let Time Domian Response Provide Additional Insight into Network Behavior", 1984

[28] Joongsuk Park, Cam Nguyen, "An Ultra wide-Band Microwave Radar Sensor for Nondestructive Evaluation of Pavement Subsurface", IEEE Sensors Journal, Vol. 5, No. 5, 2005

[29] Yanchao Zhang, Wei Liu, Yuguang Fang, “Secure Localization In Wireless Sensor Networks”, 2006

[30] Chokchai Leangsuksun Jerry Potter Stephen Scott, “A Task Graph Centroid”, 1994

[31] Akira Watanabe Osamu Tooyama, Masayuki Miyama Masahiko Yoshimoto, Junichi Akita, “An Image Sensor With Fast Extraction Of Objects’ Positions-Rough Vision Processor”, IEEE 2001

[32] Pascal Ballester, “Applications of the Hough Transform”, Astronomical Data Analysis Software and Systems III, 1994

[33] Chris Savarese, Yashesh Shroff, Greg Lawrence, “Triangulation in Ad-Hoc Networks: An Energy Efficient Solution”

[34] Qing Li, Dennis P. Nyquist, Kun-Mu Chen, Edward J. Rothwell, “Radar Target Discrimination Schemes Using Time-Domain and Frequency-Domain Methods for Reduced Data Storage”, IEEE Transactions On Antennas And Propagation, Vol. 45, No. 6, June 1997

[35] M. Matacchione, L Lo Presti, G. Olmo, “Use of Time Frequency Representation for Time Delay Estimation of Non Stationary Multicomponent Signals”

[36] Sune R.J. Axelsson, “Noise Radar Using Random Phase and Frequency Modulation” IEEE 2003

[37] A. Catovic, Z. Sahinoglu, “Hybrid TOA/RSS and TDOA/RSS Location Estimation Schemes for Short-RangeWireless Networks”, 2004

[38] Lewis Girod, “Localization - Distributed Embedded Systems” 2003

[39] Shengli Wu, Fabio Crestani, “Data Fusion with Estimated Weights”, ACM 2002

[40] Mordechai Azaria And David Hertz, “Time Delay Estimation by Generalized Cross Correlation Methods”, IEEE 1984

[41] Knapp, C.H., Carter, C.G., “ The Generalized Correlation Method for Estimation of Time Delay”, 1975

BIOGRAPHICAL INFORMATION

Kartik Trasi has been involved in graduate research at the Wave Scattering Research Center, University of Texas at Arlington. His research focused mainly on robust passive target localization in wireless and radar sensor networks. He currently working as a Wireless Systems Engineer at Cerion Inc. involved in Research and Development of 2.5G/3G Wireless Communication Technologies and software tools. The focus of the organization is core-network design and optimization for mobile networks.